TECHNICAL REPORT 90-13

RADIONUCLIDE CHAIN TRANSPORT WITH MATRIX DIFFUSION AND NON-LINEAR SORPTION

A. JAKOB
J. HADERMANN
F. RÖSEL

FEBRUARY 1990

Nagra
Nationale
Genossenschaft
für die Lagerung
radioaktiver Abfälle

Cédra
Société coopérative
nationale
pour l'entreposage
de déchets radioactifs

Cisra
Società cooperativa
nazionale
per l'immagazzinamento
di scorie radioattive

TECHNICAL REPORT 90-13

RADIONUCLIDE CHAIN TRANSPORT WITH MATRIX DIFFUSION AND NON-LINEAR SORPTION

A. JAKOB
J. HADERMANN
F. RÖSEL

FEBRUARY 1990

Parkstrasse 23 5401 Baden/Schweiz Telephon 056/20 55 11

Der vorliegende Bericht wurde im Auftrag der Nagra erstellt. Die Autoren haben ihre eigenen Ansichten und Schlussfolgerungen dargestellt. Diese müssen nicht unbedingt mit denjenigen der Nagra übereinstimmen.

Le présent rapport a été préparé sur demande de la Cédra.
Les opinions et conclusions présentées sont celles des auteurs et ne correspondent pas nécessairement à celles de la Cédra.

This report was prepared as an account of work sponsored by Nagra. The viewpoints presented and conclusions reached are those of the author(s) and do not necessarily represent those of Nagra.

Table of Contents

Vorwort

Im Rahmen des Programmes Entsorgung werden im PSI Arbeiten zur Analyse der Ausbreitung radioaktiver Elemente in geologischen Medien durchgeführt. Diese Untersuchungen werden in Zusammenarbeit und mit teilweiser finanzieller Unterstützung der Nationalen Genossenschaft für die Endlagerung radioaktiver Abfälle (NAGRA) vorgenommen. Die vorliegende Arbeit erscheint gleichzeitig als PSI–Bericht und als NAGRA Technischer Bericht.

Abstract

The present paper describes a two–dimensional model for radionuclide chain transport in inhomogeneous rock.
Advective and dispersive flux takes place in water conducting zones which may consist of a network either of tubelike veins or planar fractures. Out of these flowpaths nuclides diffuse into stagnant pore water of a spatially limited, adjacent zone (matrix diffusion). Sorption on rock surfaces is described by a non–linear isotherm. Under specific conditions matrix diffusion can be represented by an effective (non–linear) surface sorption. Radioactive decay and, in the case of a nuclide chain, ingrowth is also included in the model.
The numerical solutions of transport equations based on the method of lines are developed in detail. The advantages of this approach are the efficiency, the reliability and the general flexibility especially to include arbitrary boundary and initial conditions and arbitrary solute/rock interactions.
For ^{135}Cs we present in a comprehensive sensitivity analysis the impact of non–linear (Freundlich) sorption isotherm on break–through curves. It is shown that, provided transport times are comparable or larger than nuclide half–life, non–linear sorption may reduce concentrations at the geosphere outlet by orders of magnitude. Some results are also given for the transport of the ^{238}U chain.

Zusammenfassung

Es wird ein zweidimensionales Modell für den Transport von Radionukliden durch inhomogene Gesteine beschrieben.
Der advektive und dispersive Transport findet in wasserführenden Zonen statt, welche als Netzwerk von röhrenförmigen Adern oder planaren Spalten modelliert werden. Aus diesen Zonen heraus diffundieren die Radionuklide in das stagnierende Porenwasser einer anliegenden, räumlich begrenzten Zone von Gestein (Matrixdiffusion). Die Sorption von Radionukliden an den Gesteinsoberflächen wird durch eine nicht–lineare Isotherme beschrieben. Unter speziellen Bedingungen kann die Matrixdiffusion durch eine effektive (nicht–lineare) Oberflächensorption beschrieben werden. Radioaktiver Zerfall und, bei Kettentransport, Aufbau wird im Modell berücksichtigt.
Die numerische Lösung der Transportgleichungen beruht auf der Methode der Linien und wird im Detail entwickelt. Die Vorteile dieser Methode sind Effizienz, Zuverlässigkeit und speziell die Flexibilität in bezug auf Randbedingungen, Anfangsbedingungen und Berücksichtigung verschiedenster Formen der Nuklid/Gesteinswechselwirkung.
Für das Nuklid ^{135}Cs zeigen wir in einer umfassenden Sensitivitätsanalyse den Einfluss der nicht–linearen (Freundlich) Isotherme auf die Durchbruchkurven. Falls die Transportzeiten vergleichbar oder grösser als die Nuklidhalbwertszeiten sind, kann die Nichtlinearität der Sorptionsisotherme die Konzentrationen am Ausgang der Geosphäre um Grössenordnungen reduzieren. Für den Transport der ^{238}U–Kette werden ebenfalls einige Resultate dargestellt.

Riassunt

Nus preschantain ün model in duos dimensiuns pel transport da nuclids radioactivs tras crap na omogen.
Il transport advectiv e dispersiv ha lö aint illas zonas chi mainan aua. Quellas pon consister in ün sistem da raits in fuorma da bavröla o in sfessas planaras. La diffusiun our da las zonas maina il nuclids radioactivs ill'aua stagnanta dallas poras d'üna zona vaschina, ch'id es localmaing limitada (diffusiun da matriza). La sorpziun dals nuclids vi da las surfatschas dal crap as lascha descriver cun üna isoterma na lineara. Suot cundiziuns specialas po la diffusiun da matriza gnir rapreschentada cun üna sorpziun effectiva (na lineara) alla surfatscha. Il model resguarda tant la decadenza radioactiva co eir l'accreschimaint in cas d'ün transport da chadaina.

Las soluziuns numericas da las equaziuns da transport as basan sülla metoda da lingias es vegnan sviluppadas in detagl. Ils avantags da quista metoda sun l'efficacità, la tschertezza e specialmaing eir la flexibilità generala per quai chi reguarda las cundiziuns marginalas e quellas inizialas considerand las plü differentas fuormas d'effets vicendaivels nuclid/crap.
Pel nuclid ^{135} Cs preschantain nus in üna analisa da sensitività extaisa l'effet dall'isoterma na lineara (Freundlich) süllas curvas da prorupziun. I vain muossà, a cundiziun cha'ls temps da transport sun cumparabels o plü gronds co'ls temps da mezza valur dals nuclids in dumonda, cha la sorpziun na lineara redüa las concentraziuns illa sortida dalla geosfera per dimensiuns. Ün pêr resultats pel transport dalla chadaina dal ^{238} U vegnan eir preschantats.

Resumé

Un modèle de transport bidimensionnel de radionuclide en roche inhomogène est décrit dans ce rapport.
Le transport advectif et dispersif a lieu dans les zones conduisant l'eau qui peuvent être considérées comme un réseau de veines en forme de tubes ou de fractures planes. Les nuclides diffusent de ces zones conductrices dans l'eau stagnante des pores, en cette zone de la roche limitée dans l'espace (diffusion dans la matrice). La sorption des radionuclides à la surface de la roche est décrite par une isotherme non–linéaire.
Dans certaines conditions, la diffusion dans la matrice peut être représentée par une sorption (non–lineaire) à la surface des zones conductrices. La décroissance radioactive et, dans le cas de chaîne de décroissance, la croissance d'activité sont également prises en considération dans ce modèle.
Les solution numériques des équation de transport basées sur la méthode des lignes sont développées en détail. Les avantages de cette approche sont son efficacité, sa fiabilité et sa flexibilité en égard aux conditions limites et initiales ainsi qu'aux formes arbitraires d'interaction entre nuclide et roche.
Pour le ^{135}Cs, nous montrons par une analyse de sensitivité l'impact de la sorption non–linéaire (Freundlich) sur la combe d'écoulement. Il est démontré qu'à temps de transport comparable ou plus grand que la période du nuclide, la sorption non–linéaire peut réduire les concentrations de plusieurs ordres de grandeur à la sortie de la géosphère. Quelques resultats sont également donnés pour les nuclides de filiation de l' ^{238}U.

1 Introduction

In a safety assessment of deep radioactive waste repositories the geological barrier plays an extremely important rôle. Besides its protective function of shielding a repository from natural processes and human activities in the upper subsurface and from large water flows in aquifers, a carefully selected host rock represents a powerful migration barrier to radionuclides released from the repository and transported by circulating groundwater. The main mechanisms for retarding radionuclide transport by the flowing groundwaters are sorption on available rock surfaces and diffusion from water carrying zones into pore spaces with stagnant waters. The latter process may also contribute to safety in diluting contaminated groundwater by the fresh waters in extended pore structures of a rock matrix.

Some time ago a model for radionuclide chain transport in a dual porosity medium was presented [1] taking into account advective transport in zones of flowing waters of planar geometry (fractures) or circular geometry (veins, channels), dispersion induced by a network of such fractures or veins, diffusion into a limited space of intact rock matrix and sorption on rock surfaces represented by a linear sorption isotherm.

In the context of a safety assessment, the geometrical structures implemented in the model are adequate in view of the data available and need no further refinement at present. In fact, they are sufficiently good representations of nature not only for crystalline host rocks in northern Switzerland, where the model found its first application [2], but also for the inhomogeneous sedimentary layers of Opalinus clay and Lower Freshwater Molasse overlaying the crystalline basement [3].

However, the implementation of sorption processes in the model needs a refinement. The motivation is twofold: Firstly, increasingly sorption experiments have shown that a linear sorption isotherm is the exception rather than the rule. Modelling transport with non–linear sorption is thus a step towards more realism, which is also needed in the description of dynamic column experiments in the laboratory, which aim to test transport models. Secondly, in a safety assessment the assumption of a linear isotherm can lead to quite an unrealistic contribution of nuclides to total doses. The reason is that, for reasons of conservatism, a low sorption distribution constant corresponding to high input concentration into the geosphere has to be assumed, thus strongly underestimating retardation. Even for an equivalent porous medium with sorption on fracture surfaces, only, the nonlinearity of the isotherm can have a very strong impact on retardation and consequently on the barrier performance of a host rock [4].

The literature on transport models with nonlinear sorption is relatively scarce and, to the best of our knowledge, restricted to single porosity media. One of the reasons might be that it is not trivial to solve coupled non–linear partial differential equations and to verify the corresponding computer codes. Ref. [4] deals with safety assessment scales and solves the transport equations

by the pseudospectral method and the method of lines. Ref. [5] and especially ref. [6] discuss the effect of different sorption isotherm forms on migration and break–through curves. Ref. [6] also presents an extensive list of references. Ref. [7] deals with transport in homogeneous soils and solves the transport equation with finite difference schemes.

This paper is organised as follows:
In the next section the models for transport in idealised veins/channels and fractures are presented. Emphasis is put on the implementation of sorption. In section 3, the effect of different sorption isotherms, especially the non–linear Freundlich isotherm, on geosphere transport of radionuclides is discussed. In section 4, the effective surface sorption approximation is presented. In cases where a limited rock matrix adjacent to water carrying zones saturates rapidly with radionuclides this approximation reduces computer times appreciably. In section 5, numerical results are presented and discussed. Parameters relevant to safety assessments are used, taking as examples the migration of the fission product ^{135}Cs and of the ^{238}U chain. Section 6 summarises the conclusions and specifies some open problems. In the appendix, the salient features of the numerical solution method of the transport equation are given. In addition, the system of finite difference equations arising from the spatial discretisation, an overview to Gear's method for stiff systems of coupled ordinary differential equations and some results on numerical code verification are presented.

2 The Conceptual Model and the System of Transport Equations

In this section we present our mathematical model for describing the space–time dependent concentration of a radionuclide chain in the groundwater. The transport of the contaminant occurs by advection and hydrodynamic dispersion within water carrying zones and by molecular diffusion into and out of stagnant waters in connected pores of the surrounding rock matrix. For sorption of the radioactive tracers on available surfaces, we assume instantaneous equilibrium and a non–linear relationship between concentration in liquid and solid phase. The model also takes into account radioactive decay and – in the case of radionuclide decay chains – the ingrowth of daughters.

Geometrical aspects

For the following we consider two alternative geometries:
In the first representation (see also **Figure 1a**) we assume that the advective/dispersive flux takes place in z–direction within a fissure with constant aperture $2b$.

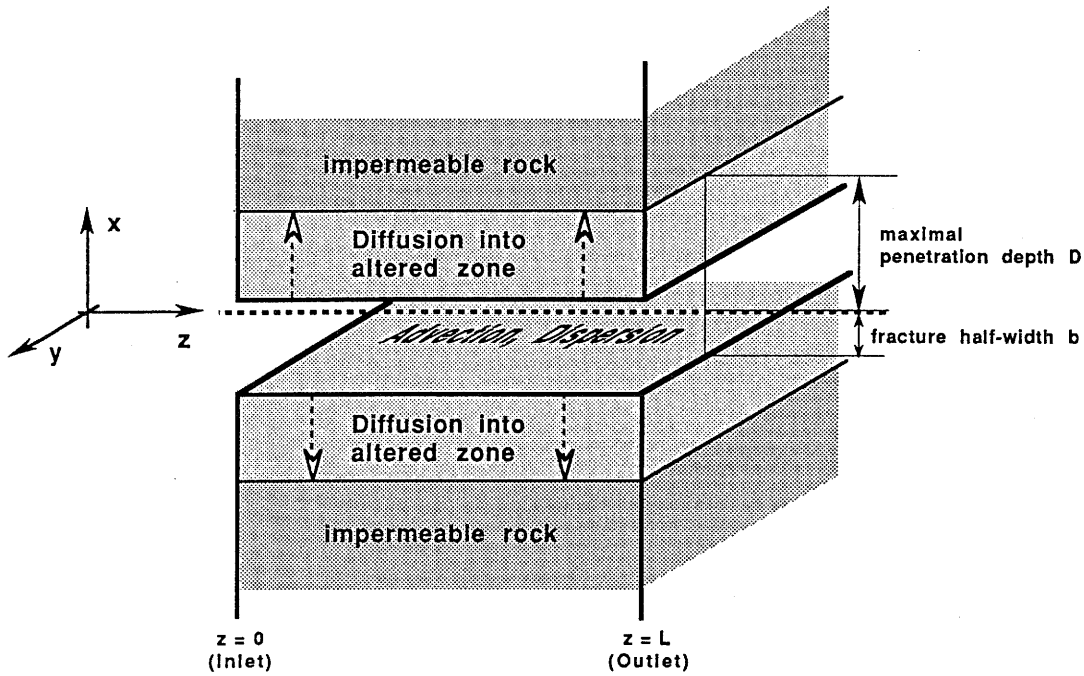

Figure 1a: The (x, z)–geometry for transport in a fracture zone.

The inlet is at $z = 0$ and we assume that the contaminant is uniformly distributed over the whole width of the fracture. Within the fracture ground water moves with a constant velocity $\vec{v}_f$.

In reality fractures are neither planar nor do they extend as single fractures over the distances to be considered. The effect of a system of interconnected fractures is simulated by a dispersion which is taken into account by a longitudinal dispersion length a_L. Sorption of the radionuclides onto fissure surfaces is governed by a non–linear isotherm.

Matrix diffusion removes the contaminant from the water conducting zone in the x–direction, perpendicular to the direction of the advective/dispersive flux, into connected porosity. The transport in the x–direction is assumed to be purely diffusive and with no advective component because of the very low hydraulic conductivity. The rock matrix accessible to diffusion is limited, be it by symmetry considerations (half the distance to the next fracture) or by a limited extent of interconnected pore spaces (limited matrix diffusion). Within the pores the nuclides sorb and the sorption isotherm may be again a non–linear one. Additionally, we assume radioactive decay and, in the case of a nuclide chain, decay of the precursor. This simple scenario for our model represents, for example, contaminant flow in fractured dykes of aplite and pegmatite in the crystalline [2] but also flow in other geological features such as "crushed zones" or larger conductive layers [3].

The alternative geometry is sketched in **Figure 1b**, where flowpaths are veins or channels and are modelled by tubes of a constant radius R. The relevant physical mechanisms are the same as specified in the previous case.

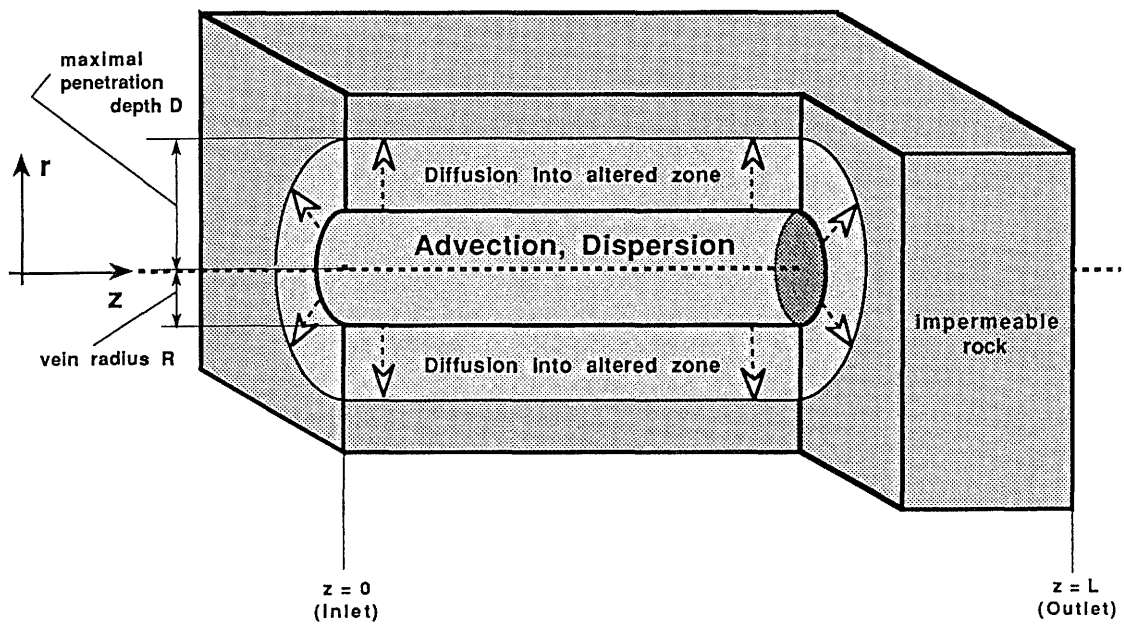

Figure 1b: Model of the (r, z)–geometry in the case of transport in veins.

Some remarks to the concept of the REV

A microscopic description of the radionuclide transport is not feasible due to the lack of knowledge on the geometrical structures. It is also not possible to describe in an exact mathematical manner all the relevant physical/chemical processes between the host rock and the moving radionuclides.

But, fortunately, we are not interested in the microscopic distribution of the contaminant and, following Bear [8], [9], the concept of the Representative Elementary Volume REV is introduced. The actual (microsopic) quantities are replaced by (macroscopic) continuum quantities by averaging over the REV. The size of such a REV strongly depends on geometry of the solid phase and represents the smallest possible volume which contains the full geometrical complexity of the system. Or in other words: The REV is this minimum volume of material over which a physical quantity can be averaged such that its value is not sensitive to small variations of the size of the REV. Practically it is not easy to determine the size of a REV and it is very site–specific. For example, for aplite/pegmatite dykes the REV comprises the fracture and the part of the surrounding rock matrix which is accessible for matrix diffusion (see **Figure 2**).

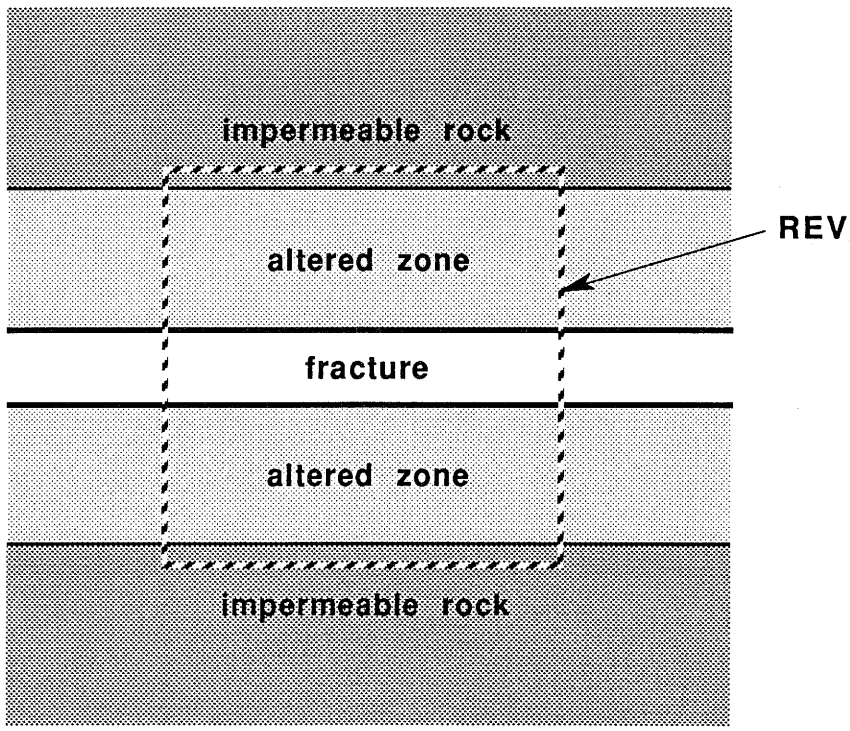

Figure 2: Schematic model for a REV in a fracture zone.

The transport equations

Following this concept the mathematical description of radioactive nuclide chain transport is based on a mass balance for the REV:

$$\frac{\partial}{\partial t}C^i_{f,tot} = \frac{\partial}{\partial t}[\epsilon_f C^i_f + \delta_f S^i_f] =$$

$$= \epsilon_f \left[D_f \frac{\partial^2 C^i_f}{\partial z^2} - v_f \frac{\partial C^i_f}{\partial z} + \begin{cases} \frac{1}{b}\epsilon_p D_p \frac{\partial C^i_p}{\partial x}\Big/_{|x| = b} \\ \frac{2}{R}\epsilon_p D_p \frac{\partial C^i_p}{\partial r}\Big/_{r = R} \end{cases} \right] + Q^{i,i-1}_f \qquad \begin{matrix} \text{(for fractures)} \\ \text{(for veins)} \end{matrix} \tag{2.1}$$

$$\frac{\partial}{\partial t}C^i_{p,tot} = \frac{\partial}{\partial t}[\epsilon_p C^i_p + (1 - \epsilon_p)\rho S^i_p] =$$

$$= \epsilon_p D_p \begin{cases} \frac{\partial^2 C^i_p}{\partial x^2} & ; \ |x| \geq b \quad \text{(for fractures)} \\ \frac{\partial^2 C^i_p}{\partial r^2} + \frac{1}{r}\frac{\partial C^i_p}{\partial r} & ; \ r \geq R \quad \text{(for veins)} \end{cases} + Q^{i,i-1}_p \tag{2.2}$$

and where:

$$\begin{aligned} Q^{i,i-1}_f &= -\lambda^i[\epsilon_f C^i_f + \delta_f S^i_f] + \lambda^{i-1}[\epsilon_f C^{i-1}_f + \delta_f S^{i-1}_f] \\ Q^{i,i-1}_p &= -\lambda^i[\epsilon_p C^i_p + (1-\epsilon_p)\rho S^i_p] + \lambda^{i-1}[\epsilon_p C^{i-1}_p + (1-\epsilon_p)\rho S^{i-1}_p] \end{aligned} \tag{2.3}$$

We used the following nomenclature:

$C^i_{f,tot}$ ... total concentration of the nuclide (i) in the water carrying zone $\left[\frac{\text{mol}}{\text{m}^3}\right]$

$C^i_{p,tot}$ ... total concentration of the nuclide (i) in the rock matrix $\left[\frac{\text{mol}}{\text{m}^3}\right]$

C^i_f ... concentration of the nuclide (i) in the flowing water $\left[\frac{\text{mol}}{\text{m}^3}\right]$

C^i_p ... concentration of the nuclide (i) in the pore water of the rock matrix $\left[\frac{\text{mol}}{\text{m}^3}\right]$

S^i_f ... concentration of the nuclide (i) on the $\begin{cases} \text{fracture} \\ \text{vein} \end{cases}$ surface $\left[\frac{\text{mol}}{\text{m}^2}\right]$

S^i_p ... concentration of the nuclide (i) on the pore surface of the rock matrix $\left[\frac{\text{mol}}{\text{kg}}\right]$

ϵ_f ... flow porosity of the $\begin{cases} \text{fracture} \\ \text{vein} \end{cases}$ $[-]$

δ_f ... sorbing surface to water volume ratio for $\begin{cases} \text{fracture} \\ \text{vein} \end{cases}$ $[\mathrm{m}^{-1}]$

D_f ... longitudinal hydrodynamic dispersion $\left[\frac{\mathrm{m}^2}{\mathrm{s}}\right]$

v_f ... water velocity $\left[\frac{\mathrm{m}}{\mathrm{s}}\right]$

b ... fracture half – width [m]

R ... vein radius [m]

ϵ_p ... effective porosity of the rock matrix [–]

D_p ... diffusion constant in the rock matrix $\left[\frac{\mathrm{m}^2}{\mathrm{s}}\right]$

λ^i ... decay constant of the nuclide (i) in a chain $1 \rightarrow 2 \rightarrow ...(\mathrm{i}-1) \rightarrow \mathrm{i} \rightarrow ...$ $[\mathrm{s}^{-1}]$

ρ ... rock density $\left[\frac{\mathrm{kg}}{\mathrm{m}^3}\right]$

(2.4)

The first (one dimensional) equation (2.1) describes the transport of the contaminant in the water conducting zones, both geometries being considered: (x, z)–cartesian geometry in the case of transport in fractures and (r, z)–cylindrical geometry for transport in veins.

The second equation (2.2) represents (one dimensional) matrix diffusion into stagnant water of the rock matrix. Only diffusion perpendicular to the direction of the fractures or veins is considered, lateral diffusion being neglected.

Both equations are coupled by the third term on the right hand side in eq. (2.1) – the diffusive flux over the boundary. The $Q_{f,p}^{i,i-1}$ in eq. (2.3) represent general net source/sink terms, specifically radioactive decay and ingrowth, in the case of a nuclide chain.

In order to calculate the time and space dependent concentrations $C_f^i(z,t)$ within the flow path and $C_p^i(x,t)$ or $C_p^i(r,t)$ in the stagnant pore water of the matrix, we have to make reasonable assumptions about the relationship between C and S.

For host rocks considered in a safety analysis, water velocities are very small and release to the geosphere extends over tens of thousands of years or more, hence sorption kinetics plays a minor rôle. Therefore, in our model we assume instantaneous sorption equilibrium and introduce the sorption isotherm:

$$S_{f,p}^i = f(C_{f,p}^i) \tag{2.5}$$

where $f(C)$ may be any function in general of different form for fractures/veins and matrix.

In section 3 we will consider specific isotherms.

Introducing eq. (2.5) into the coupled transport equations (2.1) and (2.2) we get:

$$\frac{\partial}{\partial t}C^i_{f,tot} = \epsilon_f\left[1 + \frac{\delta_f}{\epsilon_f}\frac{\partial f(C^i_f)}{\partial C^i_f}\right]\frac{\partial C^i_f}{\partial t} = \epsilon_f \cdot R_f(C^i_f)\frac{\partial C^i_f}{\partial t} =$$

$$= \epsilon_f\left[D_f\frac{\partial^2 C^i_f}{\partial z^2} - v_f\frac{\partial C^i_f}{\partial z} + \begin{cases} \frac{1}{b}\epsilon_p D_p \frac{\partial C^i_p}{\partial x}\Big/_{|x| = b} \\ \frac{2}{R}\epsilon_p D_p \frac{\partial C^i_p}{\partial r}\Big/_{r = R} \end{cases}\right] + Q^{i,i-1}_f \quad \begin{matrix} \text{(for fractures)} \\ \text{(for veins)} \end{matrix} \tag{2.6}$$

whence:

$$\frac{\partial C^i_f}{\partial t} = \frac{1}{R_f(C^i_f)}\left[a_L v_f\frac{\partial^2 C^i_f}{\partial z^2} - v_f\frac{\partial C^i_f}{\partial z} + \begin{cases} \frac{1}{b}\epsilon_p D_p \frac{\partial C^i_p}{\partial x}\Big/_{|x| = b} \\ \frac{2}{R}\epsilon_p D_p \frac{\partial C^i_p}{\partial r}\Big/_{r = R} \end{cases}\right.$$

$$\left. -\lambda^i \tilde{R}_f(C^i_f)\cdot C^i_f + \lambda^{i-1}\tilde{R}_f(C^{i-1}_f)\cdot C^{i-1}_f\right] \quad \begin{matrix} \text{(for fractures)} \\ \text{(for veins)} \end{matrix} \tag{2.7}$$

and:

$$\frac{\partial}{\partial t}C^i_{p,tot} = \epsilon_p\left[1 + \frac{1-\epsilon_p}{\epsilon_p}\rho\frac{\partial f(C^i_p)}{\partial C^i_p}\right]\frac{\partial C^i_p}{\partial t} = \epsilon_p \cdot R_p(C^i_p)\frac{\partial C^i_p}{\partial t} =$$

$$= \epsilon_p D_p \begin{cases} \frac{\partial^2 C^i_p}{\partial x^2} \\ \frac{\partial^2 C^i_p}{\partial r^2} + \frac{1}{r}\frac{\partial C^i_p}{\partial r} \end{cases} + Q^{i,i-1}_p \quad \begin{matrix} \text{(for fractures)} \\ \text{(for veins)} \end{matrix} \tag{2.8}$$

whence:

$$\frac{\partial C^i_p}{\partial t} = \frac{1}{R_p(C^i_p)}\left[D_p \begin{cases} \frac{\partial^2 C^i_p}{\partial x^2} \\ \frac{\partial^2 C^i_p}{\partial r^2} + \frac{1}{r}\frac{\partial C^i_p}{\partial r} \end{cases}\right.$$

$$\left. -\lambda^i \tilde{R}_p(C^i_p)\cdot C^i_p + \lambda^{i-1}\tilde{R}_p(C^{i-1}_p)\cdot C^{i-1}_p\right] \quad \begin{matrix} \text{(for fractures)} \\ \text{(for veins)} \end{matrix} \tag{2.9}$$

where we introduced the following abbreviations for the four concentration dependent functions, $R_f(C_f^i)$, $R_p(C_p^i)$, $\tilde{R}_f(C_f^i)$ and $\tilde{R}_p(C_p^i)$, respectively[2]:

$$R_f(C_f^i) := 1 + \frac{\delta_f}{\epsilon_f}\frac{df(C_f^i)}{dC_f^i} = \begin{cases} 1 + \frac{1}{b}\frac{df(C_f^i)}{dC_f^i} & \text{(for fractures)} \\ 1 + \frac{2}{R}\frac{df(C_f^i)}{dC_f^i} & \text{(for veins)} \end{cases} \tag{2.10}$$

and

$$R_p(C_p^i) := 1 + \frac{1-\epsilon_p}{\epsilon_p}\rho\frac{df(C_p^i)}{dC_p^i} \tag{2.11}$$

$$\tilde{R}_f(C_f^i) := 1 + \frac{\delta_f}{\epsilon_f}\frac{f(C_f^i)}{C_f^i} = \begin{cases} 1 + \frac{1}{b}\frac{f(C_f^i)}{C_f^i} & \text{(for fractures)} \\ 1 + \frac{2}{R}\frac{f(C_f^i)}{C_f^i} & \text{(for veins)} \end{cases} \tag{2.12}$$

and

$$\tilde{R}_p(C_p^i) := 1 + \frac{1-\epsilon_p}{\epsilon_p}\rho\frac{f(C_p^i)}{C_p^i} \tag{2.13}$$

Because, generally, the diffusive flux in the flow path is much smaller than the dispersive we neglect it and write:

$$D_f = a_L v_f \tag{2.14}$$

where a_L [m] is the longitudinal dispersion length.

The initial conditions are given by:

$$C_f^i(z,t) = \begin{cases} C_p^i(x,t) = 0 & |\, x \,| \geq b \\ C_p^i(r,t) & r \geq R \end{cases} \quad ; t \leq 0 \qquad \begin{matrix} \text{(for fractures)} \\ \text{(for veins)} \end{matrix} \tag{2.15}$$

assuming that the geosphere originally is free of the contaminant (It is clear that this assumption does not hold for certain nuclides like ^{235}U, ^{238}U (see also the following section (p. 16)).

The general mixed von–Neumann/Dirichlet boundary conditions are:

[2]We would like to point out that, for a linear isotherm, $R_f \equiv \tilde{R}_f$ and $R_p \equiv \tilde{R}_p$ holds, and the functions reduce to the usual retardation factors.

$$\alpha_i(z,t) \cdot C_f^i(z,t) \; + \; \beta_i(z,t) \frac{\partial C_f^i(z,t)}{\partial z} \; = \; \gamma_i(z,t) \tag{2.16}$$

for the transport equation (2.7) in the water carrying zones where $i = 1$ is for $z = 0$ and $i = 2$ for $z = L$. For the diffusion equation (2.9) we also have the general boundary conditions

$$\begin{aligned} \alpha_3(x,t) \cdot C_p^i(x,t) \; + \beta_3(x,t) \frac{\partial C_p^i(x,t)}{\partial x} \; &= \; \gamma_3(x,t) \;\; ; \mid x \mid = \; b \text{ or } D \qquad \text{(for fractures)} \\ \alpha_3'(r,t) \cdot C_p^i(r,t) \; + \beta_3'(r,t) \frac{\partial C_p^i(r,t)}{\partial r} \; &= \; \gamma_3'(r,t) \;\; ; \quad r \; = \; R \text{ or } D \qquad \text{(for veins)} \end{aligned} \tag{2.17}$$

The functions α_i, β_i and γ_i are defined by the physical problem at hand, D [m] is the maximum penetration depth into the matrix and L [m] the migration distance along a flow path. For example at the inlet ($z = 0$) we use:

$$C_f^i(z = 0, \; t > 0) \; = \; C_0^i(t) \tag{2.18}$$

where $C_0^i(t)$ is an arbitrary function of time and normally is determined by the near–field model. For the diffusion in matrix pore waters we have the following boundary conditions:

$$\left.\begin{aligned} \frac{\partial C_p^i(x,t)}{\partial x} \Big/_{|x| \, = \, D} \; &= \; 0 \\ \frac{\partial C_p^i(r,t)}{\partial r} \Big/_{r \, = \, D} \; &= \; 0 \end{aligned}\right\} \;\; ; \;\; \forall \, t \qquad \begin{aligned} &\text{(for fractures)} \\ &\text{(for veins)} \end{aligned} \tag{2.19}$$

At the interface of the water carrying zones and the rock matrix we have the continuity condition:

$$\left.\begin{aligned} C_p^i(b,t) \\ C_p^i(R,t) \end{aligned}\right\} \; = \; C_f^i(z,t); \;\; \forall \, z, \; t > 0 \qquad \begin{aligned} &\text{(for fractures)} \\ &\text{(for veins)} \end{aligned} \tag{2.20}$$

3 The Effect of Sorption on Mass Transport – Retardation

In many cases [2],[12] an important mechanism retarding nuclide migration from a repository is the diffusion of radionuclides from a water–conducting zone into pores of the rock matrix (**matrix–diffusion**), see also ref. [10], [11] and therein. There, they may be sorbed onto the surfaces of the pores and microfissures and may undergo radioactive decay. Matrix diffusion is intrinsically included in our model and we restrict the discussion in this section to sorption processes.

Sorption onto the solid phases (fracture/vein surfaces, inner matrix surfaces) constitutes the main retardation mechanism for migrating radionuclides. In general the sorption and the desorption behaviour is dependent on the element, its speciation in liquid phase, its concentration and also on the characterisation of the solid phase. Well known phenomenological relationships between concentration in the liquid phase and on the solid phase have been given (among others) by Henry, Freundlich and Langmuir (see also refs. [13], [14], [15]). For practical purposes, the underlying thermodynamical concepts are rarely helpful.

We will only present results for a Freundlich isotherm in the following sections. However, for completeness and better understanding, we shall also make some remarks about the linear and the Langmuir isotherm.

For sorption equilibrium the three different isotherms have the following form:

$$\text{a) linear isotherm :} \qquad S_l = K \cdot C \tag{3.1}$$

$$\text{b) Freundlich isotherm :} \quad S_F = K \cdot C^N \quad ; \quad N > 0 \tag{3.2}$$

$$\text{c) Langmuir isotherm :} \quad S_L = \frac{K \cdot C}{(1 + K\frac{C}{S_{max}})} = \frac{S_{max} \cdot C}{(\frac{1}{K}S_{max} + C)} \tag{3.3}$$

where K, N, S_{max} are empirical constants.

The following diagrams show schematically the $S(C)$ relationship for the three types of isotherms.

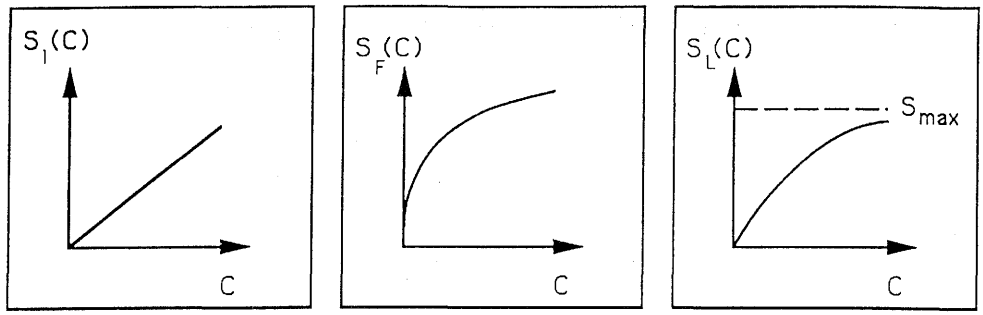

linear isotherm Freundlich isotherm Langmuir isotherm

Figure 3: Schematic diagrams for the three types of isotherms

For low concentration $C \ll S_{max}$ the Langmuir isotherm has a linear behaviour and for high concentration, $S(C)$ becomes a constant = S_{max}, the saturation concentration.
For completeness we also show schematically the three different types of retardation functions $R(C)$[3].

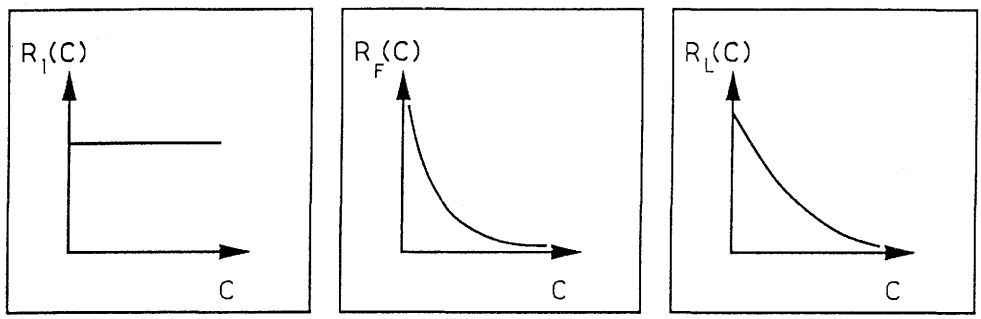

linear isotherm Freundlich isotherm Langmuir isotherm

Figure 4: $R(C)$ for the three different isotherms

In the case of a Freundlich or a Langmuir isotherm, the retardation is a function of C, hence different parts of a migrating radionuclide pulse will migrate differently and its shape will change with time even neglecting dispersive effects and matrix diffusion. As an unrealistic special feature of the Freundlich isotherm, we mention that the retardation function $R(C)$ becomes infinitely large for zero concentration. However, most of the elements have a natural stable isotope concentration C_{min} in the geosphere[4]. This is assumed to be constant in space and time.

[3]Remember: according to eqs. (2.10) and (2.11) $R(C) \propto \frac{dS(C)}{dC}$

[4]In passing we mention that, in principle, C is made up by the contributions of all isotopes of a specific element thus coupling, e.g., the different migrating Uranium isotopes. In many cases a single migrating isotope dominates.

If the radionuclide concentration is well below C_{min} the nuclide/rock interaction is determined by isotopic exchange, and hence a linear isotherm. Therefore it is sensible to assume that the retardation functions R_F, R_L are constant for $C \leq C_{min}$, avoiding, by the way, numerical problems for the Freundlich isotherm.

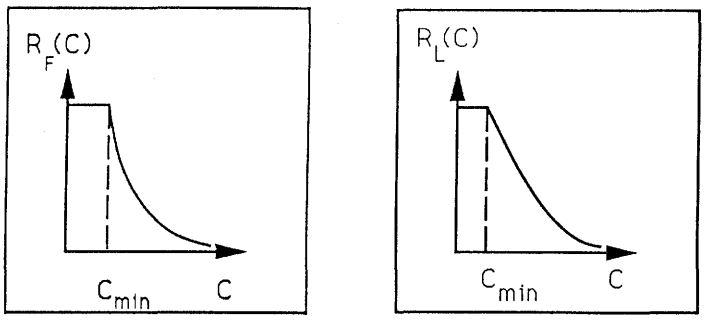

Figure 5: The "modified" Freundlich and Langmuir retardation functions, where R_F, R_L for $C \leq C_{min}$ takes a constant value. C_{min} corresponds to the natural stable isotope concentration of the element under consideration in the geosphere.

Having a look at the second derivative of $S(C)$ we see that the Freundlich, as well as the Langmuir isotherm, are concave. If C decreases, $\frac{dS}{dC}$ increases and therefore the value of the retardation function also increases. The migrating front becomes steeper – becomes a "shock front", counteracting dispersive as well as diffusive mechanisms. On the other hand the tailing part of a pulse input of a contaminant spreads out more and more. Compared to transport of radionuclides assuming a linear sorption isotherm, we expect in the case of a Freundlich sorption isotherm and a pulse input:

- a steeper front of the migrating peak ("shock front")
- a long tailing part
- a decreased maximum height
- greater transport times.

For a decaying radionuclide the percentage of fast–moving nuclides (the front) surviving decay may thus become extremely small and maximum concentrations lowered by orders of magnitude when comparing with results from a calculation with linear isotherms.

4 Effective Surface Sorption Approximation

When the diffusion into the rock matrix is sufficiently fast such that the concentration in the connected pore spaces in the matrix adjusts "instantaneously" to the concentration in the water carrying zones, diffusion into the matrix and sorption on matrix surfaces can be represented by an effective surface sorption on fracture or on vein surfaces. In ref. [1] it has been shown for transport in fractures what "instantaneously" means in quantitative terms. Therefore we assume, for the following, a priori that[5]

$$C_p^i = C_f^i \qquad \forall\, z,\ x \vee r,\ t > 0. \tag{4.1}$$

For the sorption isotherms in the fractures/veins and matrix respectively we define again:

$$S_f := f_f(C_f^i) \tag{4.2}$$

$$S_p := f_p(C_f^i) \tag{4.3}$$

For cylindrical geometry we can write down the transport equation, without loss of generality, for a nuclide which is not produced from a decaying parent:

$$\frac{\partial}{\partial t} C_{tot}^i = \left(\frac{R}{D}\right)^2 \left\{ D_f \frac{\partial^2 C_f^i}{\partial z^2} - v_f \frac{\partial C_f^i}{\partial z} \right\} - \lambda^i C_{tot}^i \tag{4.4}$$

Again, D is the maximal penetration depth for matrix diffusion, R the vein radius and $(R/D)^2$ is the ratio of volume of water carrying zone to total volume.

$$C_{tot}^i = \left(\frac{R}{D}\right)^2 C_f^i + \frac{2}{D}\left(\frac{R}{D}\right) f_f(C_f^i) + \epsilon_p \frac{D^2 - R^2}{D^2} C_f^i + \rho(1 - \epsilon_p) \frac{D^2 - R^2}{D^2} f_p(C_f^i) \tag{4.5}$$

In eq. (4.5) the first term relates to the concentration in the veins, the second to the concentration on vein surfaces; the third term is proportional to the nuclide concentration in the stagnant pore water of the matrix whereas the last term is the contribution of the concentration on the matrix pore surfaces.

Inserting eq. (4.5) into (4.4) and rearranging terms yields

$$\left\{ 1 + \frac{2}{R} \frac{df_f(C_f^i)}{dC_f^i} + \epsilon_p \frac{D^2 - R^2}{R^2} + \rho(1 - \epsilon_p) \frac{D^2 - R^2}{R^2} \frac{df_p(C_f^i)}{dC_f^i} \right\} \frac{\partial C_f^i}{\partial t} =$$

$$D_f \frac{\partial^2 C_f^i}{\partial z^2} - v_f \frac{\partial C_f^i}{\partial z} - \lambda^i \left\{ 1 + \frac{2}{R} \frac{f_f(C_f^i)}{C_f^i} + \epsilon_p \frac{D^2 - R^2}{R^2} + \rho(1 - \epsilon_p) \frac{D^2 - R^2}{R^2} \frac{f_p(C_f^i)}{C_f^i} \right\} C_f^i \tag{4.6}$$

[5] Intuitively it seems evident that eq (4.1) holds if $R_p(\overline{C_f^i}) \cdot D^2/D_p$ is a sufficiently small time, where $\overline{C_f^i}$ is an average concentration in the water carrying zones.

Comparing eqs. (4.6) and (2.6) shows that sorption on matrix surfaces can be treated as an effective surface sorption if

$$f_p(C_f^i) \;=\; \tilde{c} f_f(C_f^i) \tag{4.7}$$

where $\tilde{c}$ is an arbitrary constant. For a Freundlich isotherm, e.g., this requires $N_f = N_p$. In the expressions for $R_f(C_f^i)$ and $\tilde{R}_f(C_f^i)$, eq. (2.10) and (2.12) the following replacements have to be made on the right hand side

$$1 \longrightarrow 1 \;+\; \epsilon_p \frac{D^2 - R^2}{R^2} \tag{4.8}$$

and

$$f_f(C_f^i) \longrightarrow f_f(C_f^i) \;+\; \frac{\rho(1-\epsilon_p)}{2} \frac{(D^2 - R^2)}{R} \cdot f_p(C_f^i) \tag{4.9}$$

As a side remark we note the well known fact[6] that also non–sorbing tracers are retarded by matrix diffusion and the retardation factor $R_{m.d.}$ is given by

$$R_{m.d.} \;=\; 1 \;+\; \epsilon_p \frac{D^2 - R^2}{R^2} \tag{4.10}$$

So, for example, with values of $\epsilon_p = 0.033$, $D = 0.5$ m and $R = 5 \cdot 10^{-3}$ m from ref. [1] a retardation factor of $R_{m.d.} = 331$ is calculated.

For planar geometry of the water carrying zones the transport equation is

$$\begin{aligned} &\left\{1 \;+ \frac{1}{b}\frac{df_f(C_f^i)}{dC_f^i} \;+\; \epsilon_p \frac{D}{b} \;+\; \rho(1-\epsilon_p)\frac{D}{b}\frac{df_p(C_f^i)}{dC_f^i}\right\} \frac{\partial C_f^i}{\partial t} \;= \\ &D_f \frac{\partial^2 C_f^i}{\partial z^2} \;-\; v_f \frac{\partial C_f^i}{\partial z} \;-\; \lambda^i \left\{1 \;+\; \frac{1}{b}\frac{f_f(C_f^i)}{C_f^i} \;+\; \epsilon_p \frac{D}{b} \;+\; \rho(1-\epsilon_p)\frac{D}{b}\frac{f_p(C_f^i)}{C_f^i}\right\} C_f^i \end{aligned} \tag{4.11}$$

Again, eq. (4.7) is a necessary condition for an effective surface sorption approximation. In the expressions for $R_f(C_f)$ and $\tilde{R}_f(C_f^i)$, eqs. (2.10) and (2.12) the following replacements now have to be made

$$1 \longrightarrow 1 \;+\; \epsilon_p \frac{D}{b} \tag{4.12}$$

[6]This effect is also important for dating groundwaters with "ideal" tracers ([16], [17], [18]) and has especially large consequences for radioactive tracers when half–lives are smaller than tracer transport times.

and

$$f_f(C_f^i) \longrightarrow f_f(C_f^i) \; + \; \rho(1-\epsilon)D \cdot f_p(C_f^i) \tag{4.13}$$

Inspecting eqs. (4.8), (4.9), (4.12) and (4.13) one will recognize that, besides the magnitude of sorption given by the isotherm $f_p(C_f^i)$, it is the ratio of matrix pore volume to water carrying zone's volume which determines retardation by matrix diffusion. Without knowing the maximal penetration depth D little can be said whether vein or fracture flow systems are more conservative in a repository safety analysis.

We have shown under which conditions, assuming equilibrium (eq. (4.1)), matrix diffusion can be approximated by an effective surface sorption. The advantage is a massive reduction in computer time and space, especially for a large number of scoping calculations. To what extent assumption (4.1) is fulfilled remains a question difficult to answer. However, it is always possible to make a conservative estimate of a maximal penetration depth D.

5 Results and Discussion

In this section we present numerical results for the solution of the equations presented in the previous sections.

For the choice of the input parameters we take into account two considerations:

1. the parameters should clearly show the impact of the non–linear sorption isotherm on break–through curves and
2. the results should be relevant to a safety assessment of deep geological disposal.

For high–level radioactive waste one option is disposal into the crystalline basement of northern Switzerland. (The investigations have recently been extended to overlaying sedimentary rocks.) A comprehensive safety analysis has been performed some years ago [2]. Therefore, our calculations will refer to this analysis. The selection of radionuclides was influenced by recently documented sorption data from uranium and cesium [19], [20] from batch sorption and, in the case of uranium, also from a dynamic experiment [21]. Both, U and Cs, exhibit a non–linear sorption behaviour. The most important reason for choosing ^{135}Cs is the fact, that this nuclide made up 95 % of the total dose to man [2], assuming a conservatively chosen linear sorption isotherm. Considering the more realistic (non–linear) sorption behaviour of ^{135}Cs, a considerably lower dose to man is expected.
Therefore, as a starting point and with the exception of sorption data, we take again the parameters of ref. [2] for the fission product ^{135}Cs and for the actinide chain ^{238}U $\rightarrow$ ^{234}U $\rightarrow$ ^{230}Th. Nuclide dependent base–case parameters are listed in Table 1 whereas all the other input parameters are shown in Table 2.

	units	^{135}Cs	^{238}U	^{234}U	^{230}Th
Total Inventory	[mol]	$1.88 \cdot 10^{4}$	$4.69 \cdot 10^{4}$	$7.35 \cdot 10^{1}$	0.289
Solubility limit[a]	[mol/m^3]	high	$2.5 \cdot 10^{-4}$	$2.5 \cdot 10^{-4}$	$1.6 \cdot 10^{-3}$
Half–life $T^i_{1/2}$ of nuclide i	[y]	$2.30 \cdot 10^{6}$	$4.468 \cdot 10^{9}$	$2.445 \cdot 10^{5}$	$7.70 \cdot 10^{4}$
Leach–time T^i_L of nuclide i	[y]	$1.55 \cdot 10^{5}$	$5.0 \cdot 10^{7}$	$5.0 \cdot 10^{7}$	$5.0 \cdot 10^{7}$
Minimum concentration C_{min}	[mol/m^3]	$1.0 \cdot 10^{-6}$	$1.68 \cdot 10^{-5}$	–	–
Distribution constant in the fracture/vein K^i_a	[m]	[b]	$4.61 \cdot 10^{-3}$	$4.61 \cdot 10^{-3}$	$1.74 \cdot 10^{-2}$
Retentionfactor in the fracture/vein R^i_f	[–]	1.0	93.2	93.2	350
Distribution constant in the matrix K^i_d	[m^3/kg]	$3.0 \cdot 10^{-2}$	0.264	0.264	1.00
Retentionfactor in the matrix R^i_p	[–]	$2.30 \cdot 10^{3}$	$2.03 \cdot 10^{4}$	$2.03 \cdot 10^{4}$	$7.67 \cdot 10^{4}$
Freundlich coefficient in the fracture/vein K^i_f	[mol$^{1-N^i_f}$m$^{3N^i_f-2}$]	[b]	$2.72 \cdot 10^{-4}$	[c]	[c]
Freundlich exponent in the fracture/vein N^i_f	[–]	[b]	0.66	[c]	[c]
Freundlich coefficient in the matrix K^i_p	[mol$^{1-N^i_p}$ m$^{3N^i_p}$/kg]	$5.0 \cdot 10^{-2}$	$1.56 \cdot 10^{-2}$	[c]	[c]
Freundlich exponent in the matrix N^i_p	[–]	0.70	0.66	[c]	[c]

[a] Note: Values given are total concentrations for the element and shared between isotopes.
[b] Sorption on fracture/vein surfaces is neglected
[c] A linear isotherm is used for these isotopes (see text).

Table 1: Nuclide dependent input parameters (the total inventories and solubility limits are taken from [2] and are given for completeness). Freundlich parameters are base case data ([19], [20], private communications from B. Baeyens, B. Ruegger and T.T. Vandergraaf).

	units	for fractures	for veins
Site characterisation and nuclide independent parameters:			
Migration distance L	[m]	500	
Water velocity v_f	[m/y]	0.473	6.03
Dispersion length a_L	[m]	50	
Diffusion constant of altered zone D_p	[m^2/s]	$1.515 \cdot 10^{-11}$	
Porosity of altered zone ϵ_p	[–]	$3.3 \cdot 10^{-2}$	
Density of altered zone $\overline{\rho} = \rho(1-\epsilon_p)$	[kg/m^3]	2530	
Water flow through the repository Q_L	[m^3/y]	4.2	
Hydraulic conductivity K	[m/s]	$1.25 \cdot 10^{-9}$	
Hydraulic gradient $\nabla\Phi$	[–]	0.012	
Fracture frequency n_f; vein frequency n_v	[m^{-1}]; [m^{-2}]	10	1
Fracture half–width b; vein radius R	[m]	$5 \cdot 10^{-5}$	$5 \cdot 10^{-3}$
Maximal penetration depth D	[m]	10^{-3}	0.5
Boundary conditions:		α_i β_i γ_i	
Up–stream $(i=1)$		1 0 1	
Down–stream$(i=2)$[a]		1 0 0	
Release scenario:		Reference [22]	
Integration data:			
Order of the interpolation polynomial in flow direction		3	3
Number of discretisation points in flow direction		26 (equidistant)	31 (equidistant)
Order of the interpolation polynomial in matrix–diffusion direction		3	3
Number of discretisation points in matrix–diffusion direction		15 (equidistant)	58 (**not** equidistant)

[a] This down–stream boundary condition represents a strong dilution of the contaminant by an overlaying aquifer.

Table 2: Base case input parameters for both alternative geometries (Parameters are from [2]).

At the inlet, the input (boundary) concentration is given by the following expression:

$$C_f^i(z=0,t) \;:=\; C_0^i(t) \;=\; \frac{R^i(t)}{Q_L} \tag{5.1}$$

where $R^i(t)$ is the (normally) time–dependent release rate of nuclide i into the geosphere. It is taken from [22] and shown for completeness in **Figure 6.**

Q_L is the total water flow through the repository, assumed to be 4.2 m^3/y:

$$Q_L \;=\; \epsilon \cdot v_f \cdot F \tag{5.2}$$

where ϵ [−] is the average porosity of the repository region, F [m^2] is the repository cross–section and v_f is the water velocity [m/y].
At the down–stream boundary, the results of the calculations are presented as normalised nuclide flows, defined by:

$$\begin{aligned} \frac{J_{tot}(z=L,t)}{Q_L} := J_{norm}(z=L,t) \;&=\; \frac{-\epsilon \cdot v_f \cdot F \cdot a_L \left.\dfrac{\partial C_f^i}{\partial z}\right|_{z=L}}{\epsilon \cdot v_f \cdot F} \\ &= -a_L \left.\frac{\partial C_f^i}{\partial z}\right|_{z=L} \end{aligned} \tag{5.3}$$

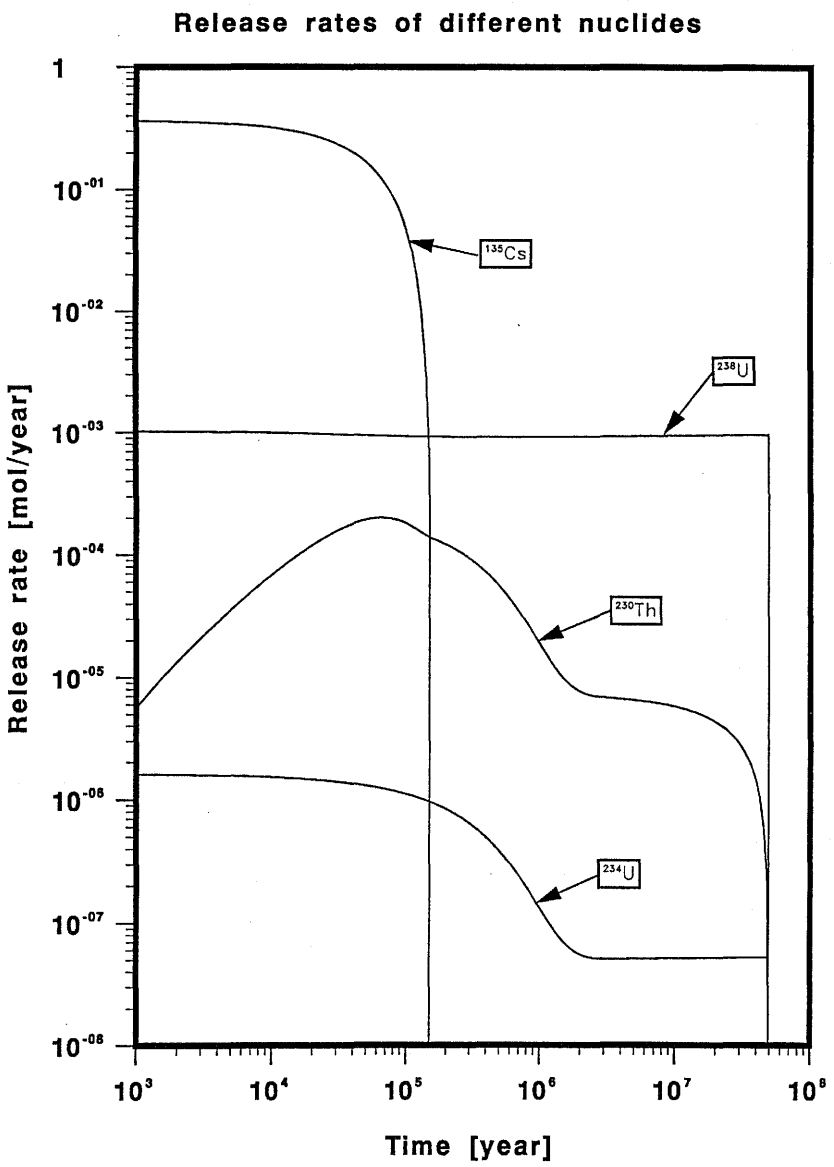

Figure 6: Release rates into the geosphere for ^{135}Cs, ^{238}U, ^{234}U, ^{230}Th as a function of time. (The canister life–time is assumed to be 1000 years). From [22].

Effects of the spatial discretisation

To test the convergence behaviour of the spatial discretisation in the flow and matrix diffusion directions we have done serveral calculations for fracture flow and vein flow systems. The starting point for these investigations are the base case integration data given in Table 2.

The effect of different orders of the local truncation error of the interpolation polynomial in vein flow is shown in **Figure 7**. Increasing the order from 3 to 5, the peak maximum decreases by less than about 20 % and the slope of the break–through curve changes slightly. To keep computer time low in the following calculations, the order is fixed to 3.

Figure 8 shows break–through curves of ^{135}Cs for different mesh sizes in vein flow. Δz is either 20 m (26 discretisation points), $16.\overline{6}...$ m (31 discretisation points) or 12.5 m (41 discretisation points). The effect on peak maximum is only small and we therefore fixed the discretisation number for the following vein flow calculations to 31, limiting thus the size of the coupling matrix.

In an analogous way, we estimated the influence of different orders of the interpolation polynomial in the matrix diffusion direction (**Figure 9**). There is essentially no difference between a second order and a fourth order correct scheme.

The effect of different numbers of discretisation points in matrix diffusion direction is shown in **Figure 10**. Plotted are again break–through curves for ^{135}Cs for the vein flow. From bottom to top, the curves represent calculations with M = 30, 40, 50 discretisation points. The last curve (M = 50, solid line) coincides with that for M = 58 discretisation points. In the case of a vein flow system the discretisation points are not equidistantly distributed in matrix diffusion direction. The coordinate is subdivided into groups. Within a group, discretisation is equidistant. With increasing distance from the water conducting zone, the size of the discretisation interval increases from group to group.

Analogous convergence tests have been done for the fracture flow system and one gets similar results. This system is somewhat less sensitive to discretisation in matrix flow direction. We do not present specific results but refer to Table 2 where the specific integration data are listed.

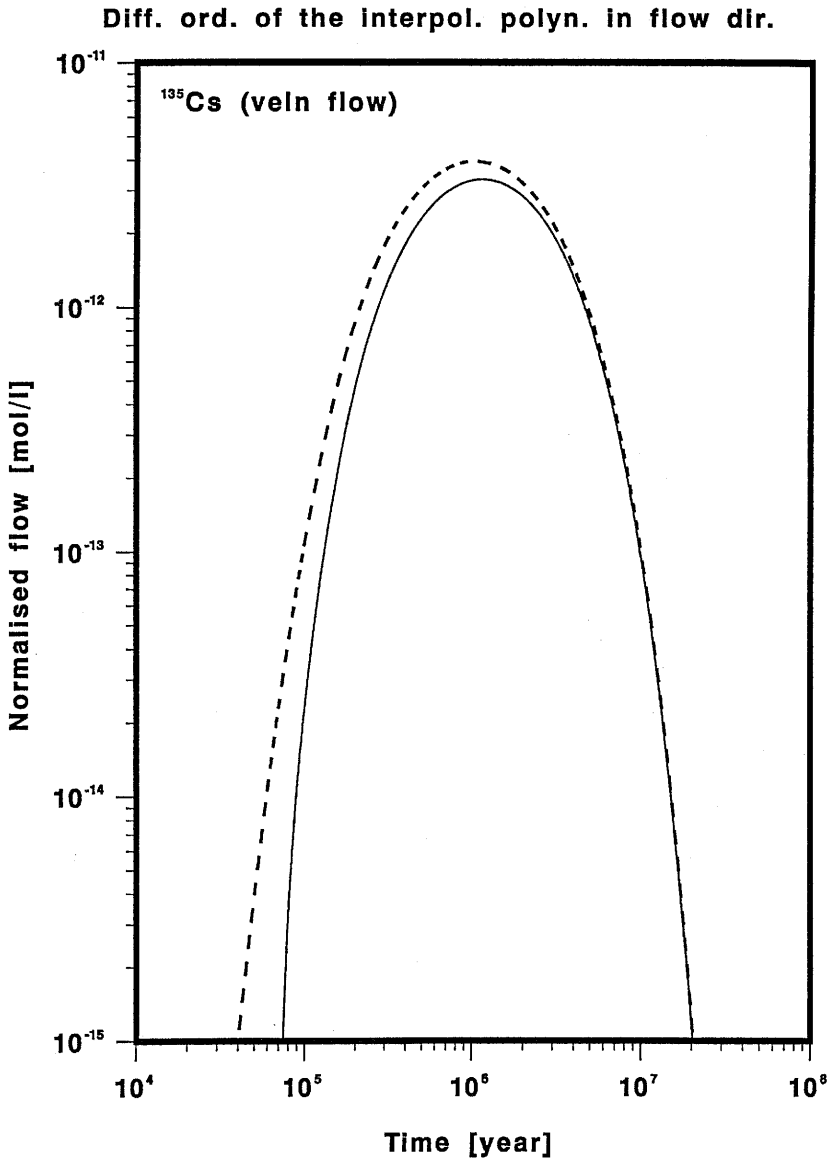

Figure 7: Effect of different order of the interpolation polynomial on the break–through curve for ^{135}Cs for a vein flow system. The dashed line is a calculation with an order 3 of the local truncation error, whereas the full line represents that of order 5. All the other parameters are those of the base case.

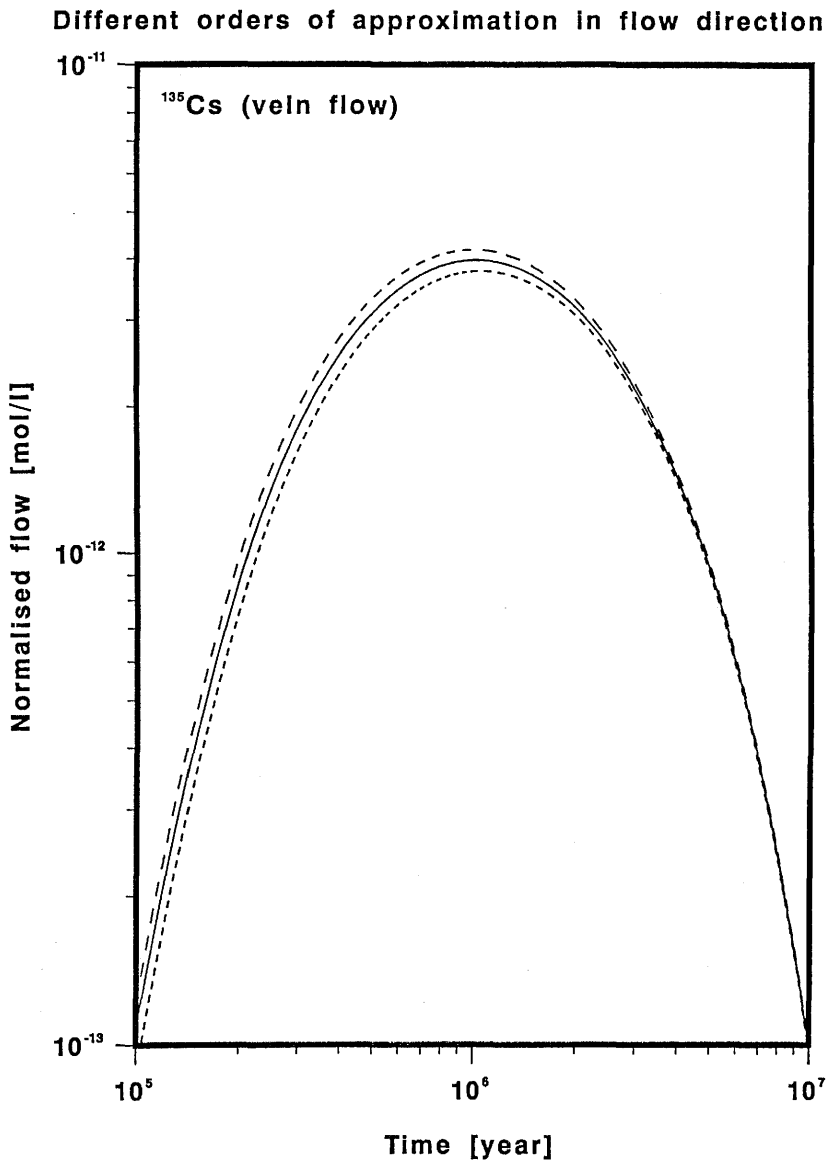

Figure 8: Normalised flow as a function of time for ^{135}Cs for a vein flow system for various mesh sizes in flow direction: – – – 26 discretisation points; —— 31 discretisation points; - - - 41 discretisation points. All the other parameters are those of the base case.

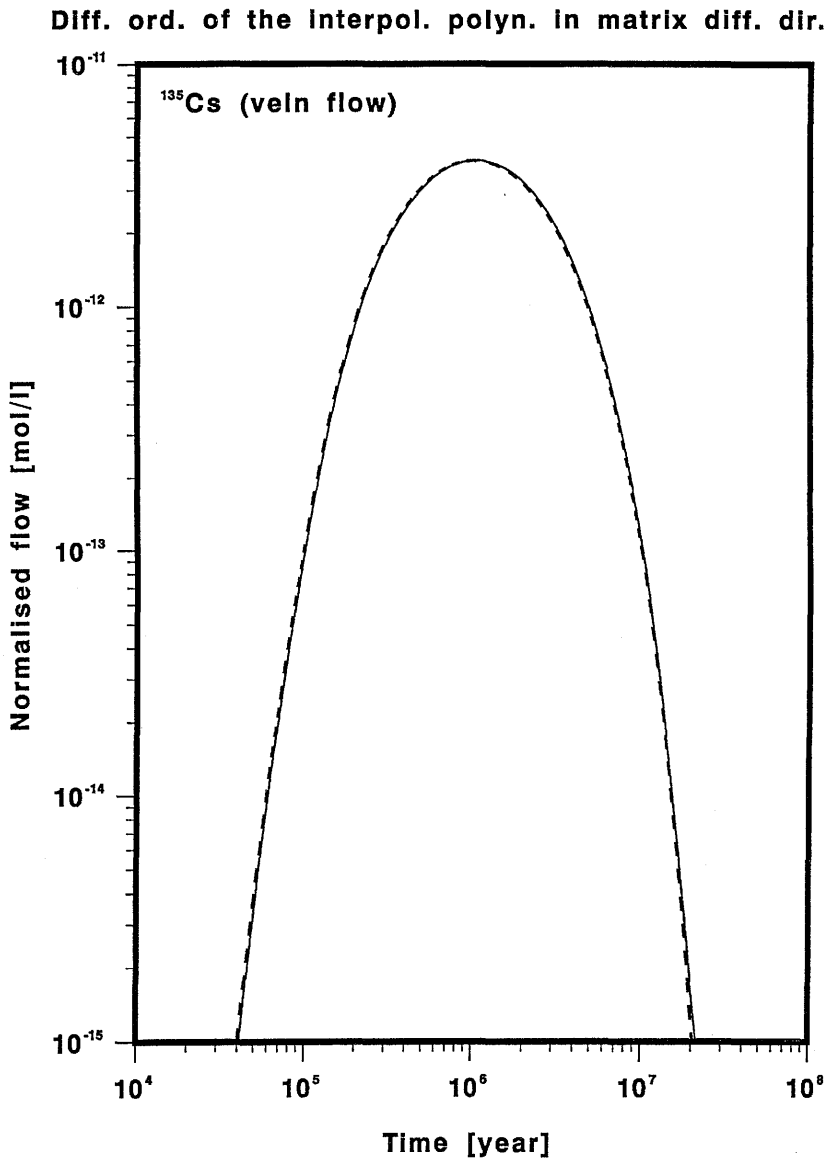

Figure 9: Effect of different orders of the interpolation polynomial in matrix diffusion direction on break–through curves for ^{135}Cs for a vein flow system (– – – second order correct scheme; —— fourth order correct scheme.)

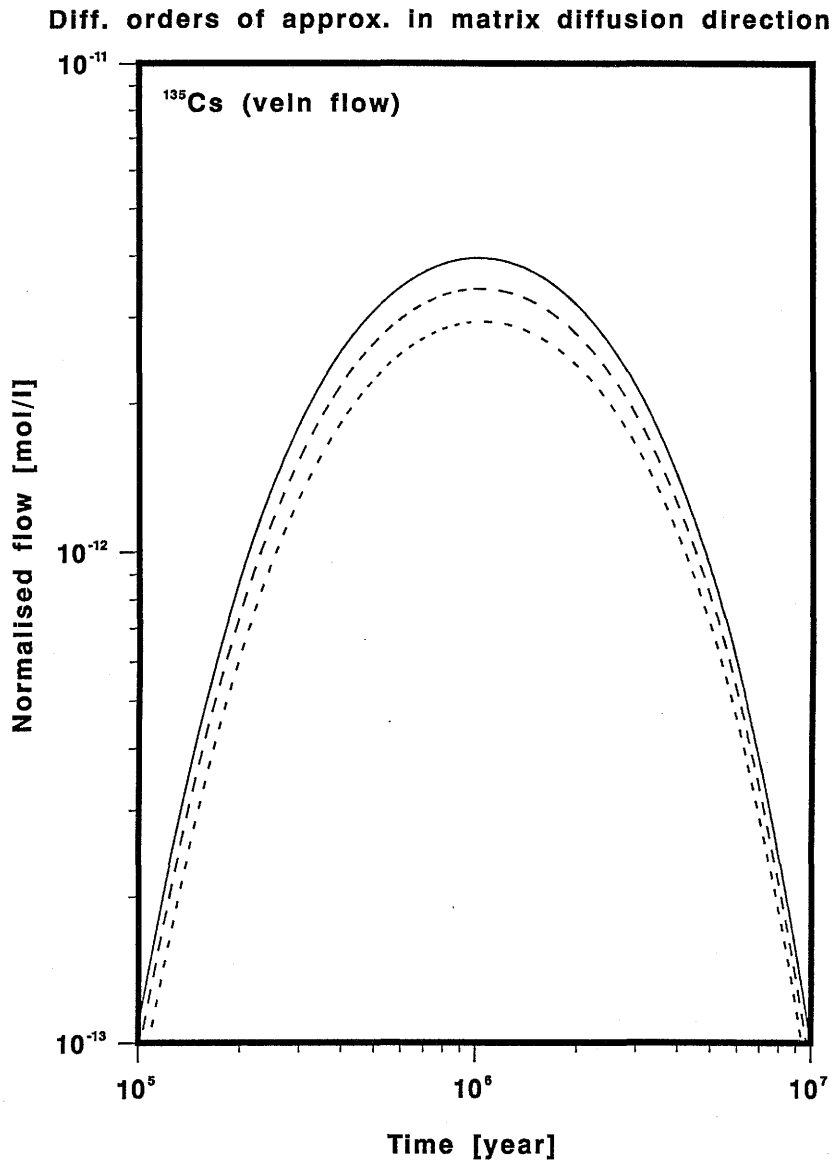

Figure 10: Normalised flow as a function of time for ^{135}Cs for a vein flow system. The curves show the effect of different numbers of (not equidistantly distributed) discretisation points. From bottom to top: M = 30, 40, 50 and 58. The calculations for M = 50 and M = 58 give identical results (solid line).

5.1 Fracture flow system

In this subsection we present results for ^{135}Cs transport in a fracture flow system. The base case parameters are specified in Tables 1 and 2.

Consideration of the non–linear sorption behaviour of cesium has a strong impact on nuclide outflow from the host rock. However, the magnitude is largely dependent on the background concentration of natural cesium in the groundwaters. For crystalline waters natural cesium concentrations from detection limit up to around 10^{-5} mol/l have been given [23], [24]. The upper values are measured in higher mineralised waters. In order to see the full impact of a non–linear isotherm we have chosen a base case value at the lower end, $C_{min} = 10^{-9}$ mol/l, and varied the parameter in a broad range. This is illustrated in **Figure 11**. The lower this natural concentration, the larger the concentration range with non–linear sorption, the steeper the front of migrating ^{135}Cs and the less survival of fast moving nuclides: Hence, the variation of nuclide flow over about six orders of magnitude. Even for a high natural cesium concentration, consideration of the non–linearity of sorption reduces outflow when compared with the result with a linear isotherm sorption coefficient chosen according to the maximum input concentration of $8.6 \cdot 10^{-5}$ mol/l. In that case, most of the ^{135}Cs nuclei survive transport. Also shown in Figure 11 is the excellent agreement of the effective surface sorption approximation with the full two–dimensional calculation. This is a consequence of the very limited volume of available rock matrix for diffusion and the rapid equilibration between matrix pore and fracture waters.

Figure 12 shows the dependence on the Freundlich coefficient for sorption in the matrix. For the lower value of K_p, retardation is small and most nuclides survive transport. For the higher value of K_p, retardation is roughly an order of magnitude larger and transport times are large compared to half–life. Again, the effective surface sorption approach constitutes an excellent approximation.

When transport times are large compared to half–life, the magnitude of the Freundlich exponent N_p becomes extremely important (**Figure 13**). For lower N_p, with a marked non–linearity, the migration fronts are steeper and the percentage of fast moving nuclides much lower. Hence, with a decrease of the Freundlich exponent by 10% one gets a reduction of outflow by five orders of magnitude. Again, the effective surface sorption approximation is an excellent approximation for the reasons mentioned above.

The retardation for transport in the fracture flow system is strongly dependent on the matrix volume available for diffusion and sorption. This is shown in **Figure 14**. Here, the calculations were performed with a low Freundlich parameter K_p since no outflow results for the base case K_p and maximum penetration depths $D \geq 0.01$ m. For the values leading to the results of Figure 14,

the matrix is rapidly saturated with ^{135}Cs and, hence, the effective surface approximation is an excellent approach. Clearly then, the retardation is directly proportional to the maximum penetration depth D and, for residence times larger than half–live, a strong dependency of maximal outflow on D results.

Keeping all other parameters fixed the residence time is directly proportional to the migration distance L if the rock matrix is saturated. This is the case for the results presented in **Figure 15**. In these calculations the Peclet number L/a_L was held constant. Smaller dispersivities and longer transport paths, both, lead to a strong decrease of nuclide outflow if residence times are large compared to half–life, as is here the case.

A similar influence on nuclide outflow results from a variation of water velocity v_f (**Figure 16**). The hydraulic conductivity K has been increased up to two orders of magnitude from the base case keeping hydraulic gradient and flow porosity constant. For the highest water velocity, all of the ^{135}Cs nuclei survive transport and peak outflow almost corresponds to peak inflow. The peak reduction for the intermediate water velocity results to a larger extent from increased dispersion when residence time increases and to a lesser extent from radioactive decay. For the base case water velocity, radioactive decay becomes extremely important.

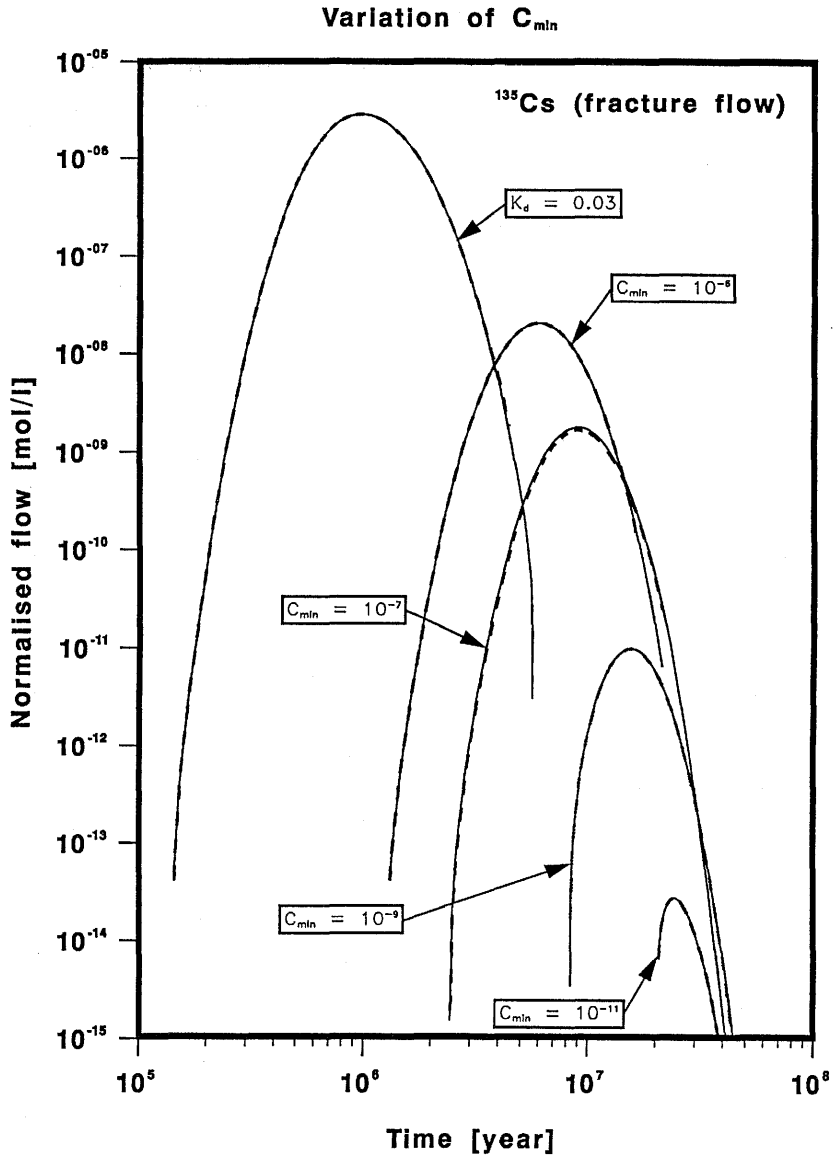

Figure 11: ^{135}Cs nuclide flow after a migration distance of 500 m normalised to a water flow of 4.2 m^3/y as a function of time after canister failure. Presented are the results for transport in the fractured aplite/pegmatite dykes. The full lines correspond to a 2D calculation and the dashed lines to the effective surface sorption approximation. The parameters are those of the base case (Table 1 and 2) except for the concentration C_{min} [mol/l] of stable cesium in the groundwater, whose values are indicated in the figure. For comparison purposes, a calculation with a linear sorption isotherm is also shown assuming a distribution constant K_d [m^3/kg] corresponding to a high ^{135}Cs input concentration.

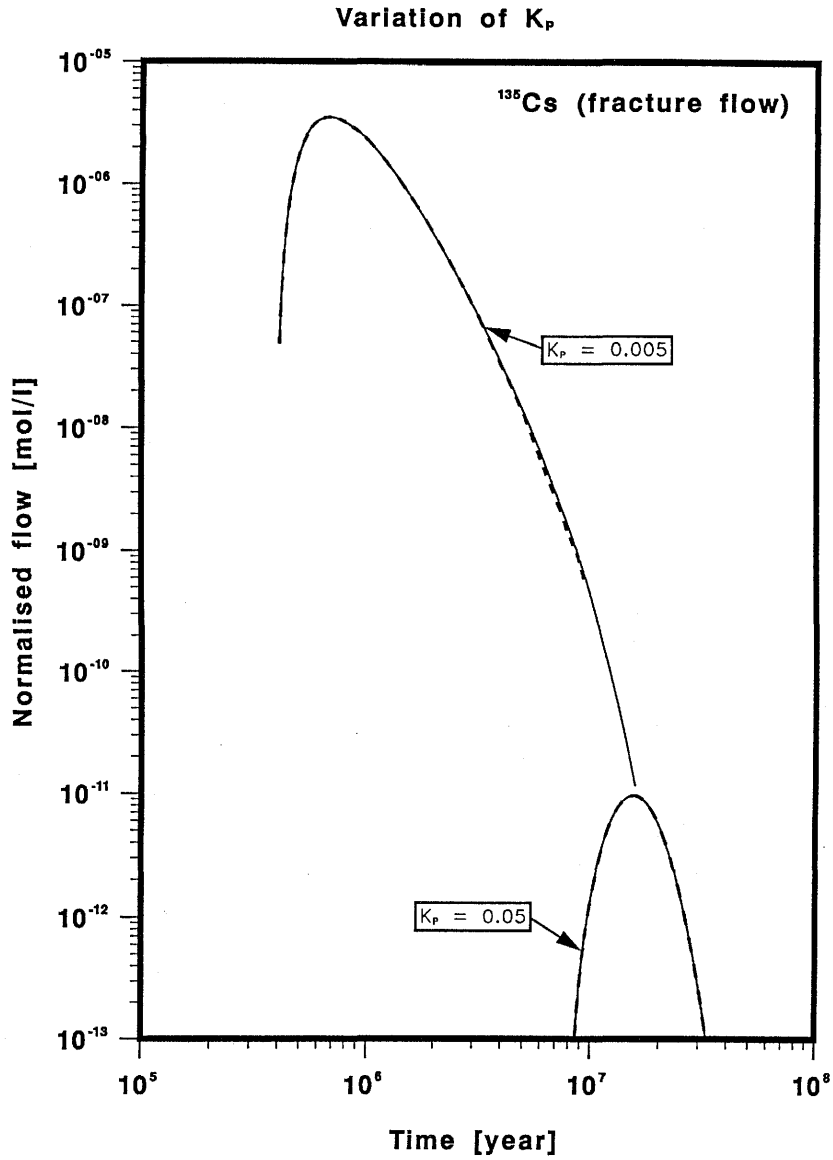

Figure 12: The same as Figure 11. The parameters are those of the base case except the Freundlich sorption coefficient K_p [mol$^{0.3}$m$^{2.1}$/kg] whose value is indicated in the figure.

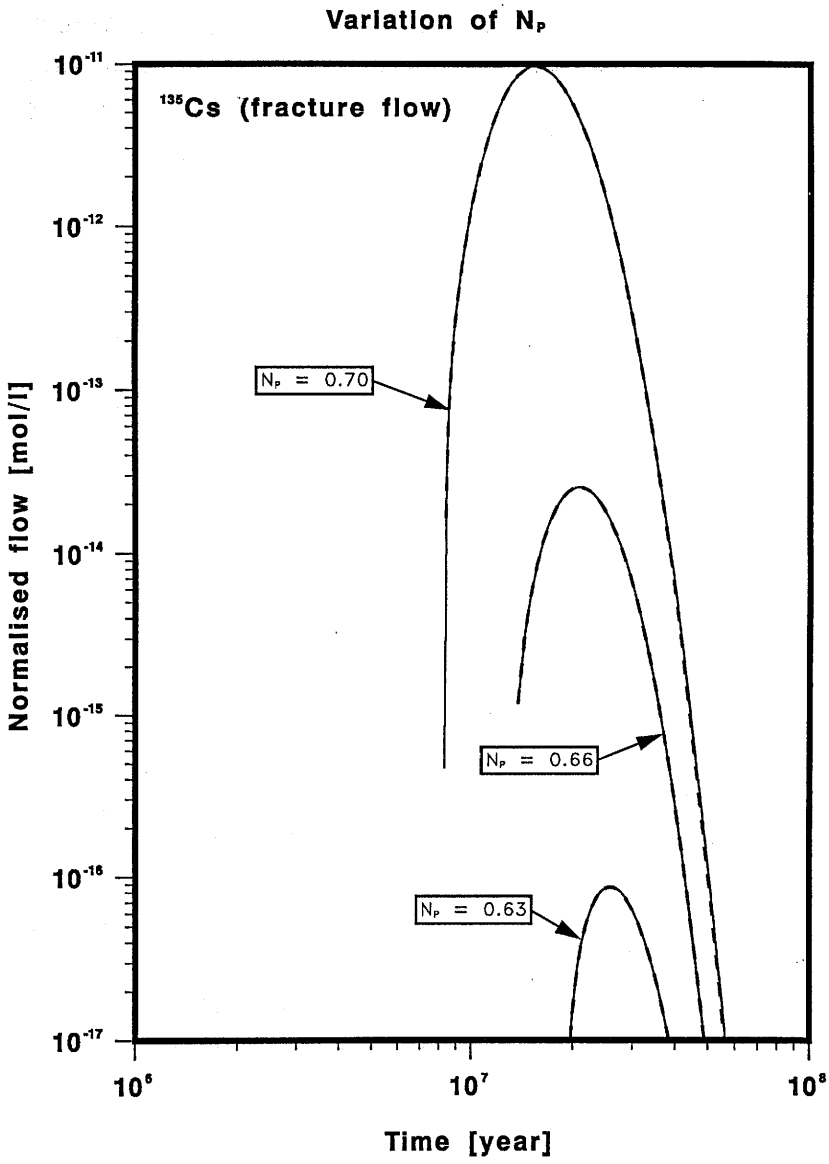

Figure 13: The same as Figure 11. The parameters are those of the base case with the exception of the Freundlich exponent N_p whose values are indicated in the figure.

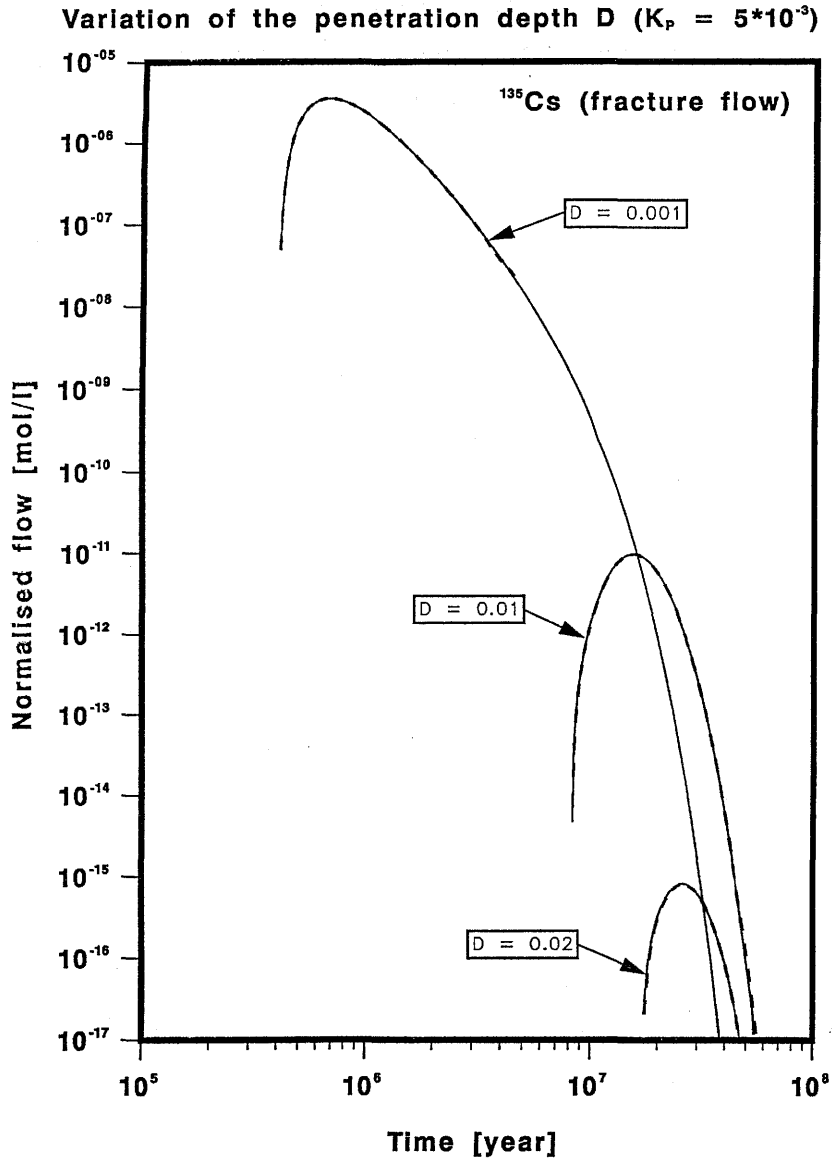

Figure 14: The same as Figure 11. The parameters are those of the base case except the Freundlich coefficient for sorption in the matrix ($K_p = 5 \cdot 10^{-3}$ mol$^{0.3}$m$^{2.1}$/kg) and the maximum penetration depth into the matrix D [m] whose values are indicated in the figure.

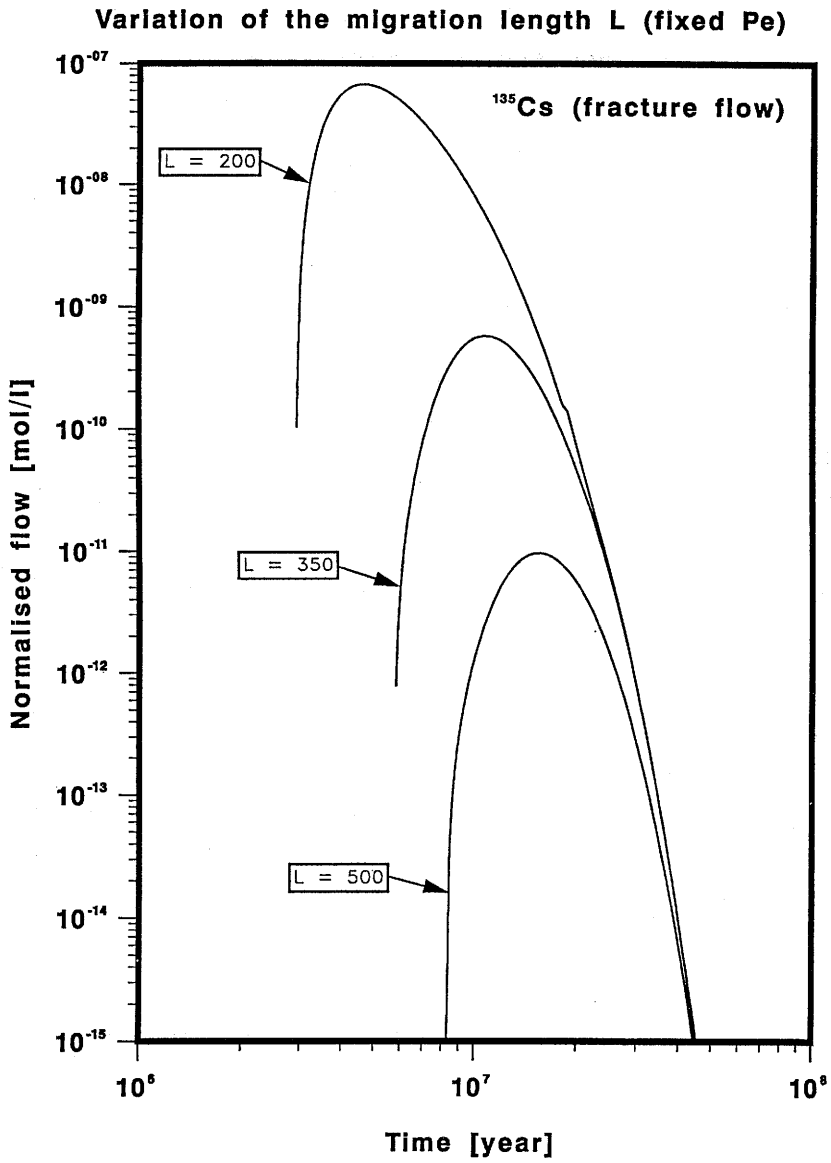

Figure 15: The same as Figure 11. The parameters are those of the base case except the migration distance L [m] whose values are indicated in the figure. The Peclet number L/a_L is fixed at the value of 10 for all three calculations.

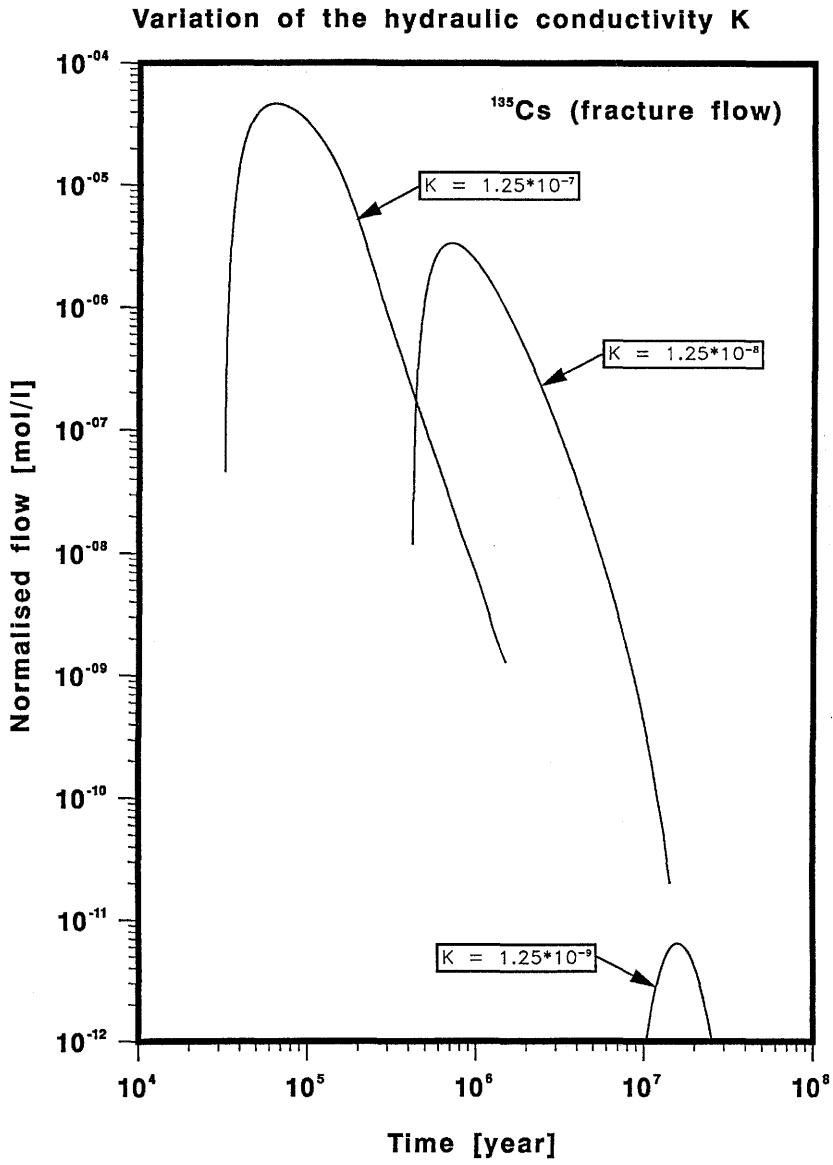

Figure 16: The same as Figure 11. The parameters are those of the base case except the hydraulic conductivity of the water carrying fractures whose values K [m/s] are indicated in the figure.

5.2 Vein flow system

The results presented in this subsection (figures 17 to 22) illustrate the main features of geosphere transport in a (r, z)–geometry. Again transport of ^{135}Cs is taken as an example and the impact of some parameter variations is investigated.

Figure 17 shows the effect of varying the natural cesium concentration on the break–through. On a lower outflow level – because available rock mass for matrix diffusion is much larger – the effect is less pronounced than for fracture flow (see figure 11). Loosely speaking, the nuclide outflow is determined by nuclides transported mainly in the veins and not the bulk of nuclides, which diffuse into and sorb in the rock matrix decaying there to insignificance. This can be seen in **Figure 18** where, for interpretation purposes, the radioactive decay has been switched off (dashed line) and the strong retardation potential of matrix diffusion as well as the effect of decay (full lines) is clearly seen. In **Figure 17**, again, the results taking into account non–linear sorption are compared to the corresponding results for a linear isotherm. This curve led to the base case dose calculation in "Project Gewähr 1985" [2, fig. 14-1]. It should be noted that consideration of a non–linear isotherm for ^{135} Cs reduces total doses in that safety assessment by a factor of 25 even for the large natural cesium background of 10^{-6} mol/l, and the contribution of cesium to almost negligible amounts.

In **Figure 19** the effect of varying the Freundlich coefficient on nuclide flow is presented. Again, for vein flow the impact is less pronounced on a lower outflow level compared to fracture flow (Figure 12). The reasons are the same as discussed above: The main portion of nuclides diffusing into and out of the matrix decay to insignificance. The same situation is seen when varying the Freundlich exponent (**Figure 20**) and comparing to Figure 13.
For practical applications in safety assessments, it is pleasing to see that the parameter dependencies are much less for vein flow than for fracture flow. However, this is mainly a consequence of the much larger matrix pore volume available for diffusion in the first flow system: The overwhelming majority of cesium nuclides diffuse into the rock matrix and decay there. The kind of sorption mechanism in the matrix plays little rôle and is felt in the geosphere outflow indirectly, only, through the coupling of the two transport equations.

Figure 21 presents the influence of maximal penetration depth for diffusion into the rock matrix. For the two smallest values of D, the peak value is determined by nuclides moving into and out of the matrix whereas for larger penetration depths the breakthrough is dominated by fast moving nuclides in the water carrying zones (see discussion above). When comparing to Figure 14, the main difference to the fracture flow system can bee seen: For vein flow the effect of matrix diffusion on nuclide outflow is limited and reaches an asymptotic value. The reason

is the totally different geometry. So, for fracture flow, the volume available for diffusion is directly proportional to the maximal penetration depth; for vein flow this volume increases with the square of the maximal penetration depth and the diffusion equation has a totally different structure. For the smallest value of D, the effective surface sorption approach constitutes a good approximation but for larger values of D the matrix is not sufficiently rapidly saturated with ^{135}Cs and, consequently the effective surface sorption approximation fails.

In **Figure 22**, the dependence on effective diffusion constant D_e is depicted. A lower value of D_e than the base case value strongly restricts the effect of matrix diffusion, whereas for a higher value more of the rock matrix is saturated more rapidly and the outflow values decrease to insignificance.

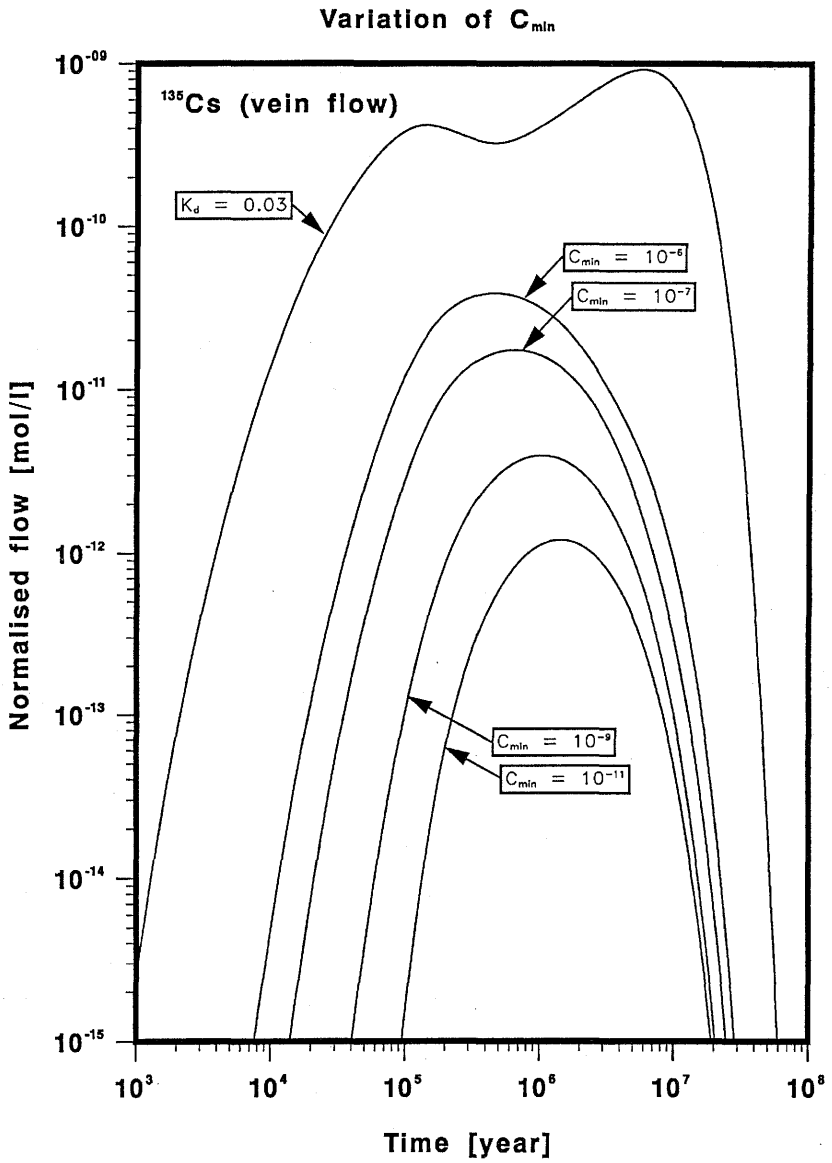

Figure 17: ^{135}Cs nuclide flow after a migration distance of 500 m normalized to a water flow of 4.2 m^3/y as a function of time after canister failure. Presented are the results for transport in kakirite veins. The parameters are those of the base case (Tables 1 and 2) except for the concentration C_{min} [mol/l] of stable cesium in the groundwater, whose values are indicated in the figure. For comparison purposes, a calculation with a linear isotherm is also shown assuming a distribution constant K_d [m^3/kg] corresponding to a high ^{135}Cs input concentration.

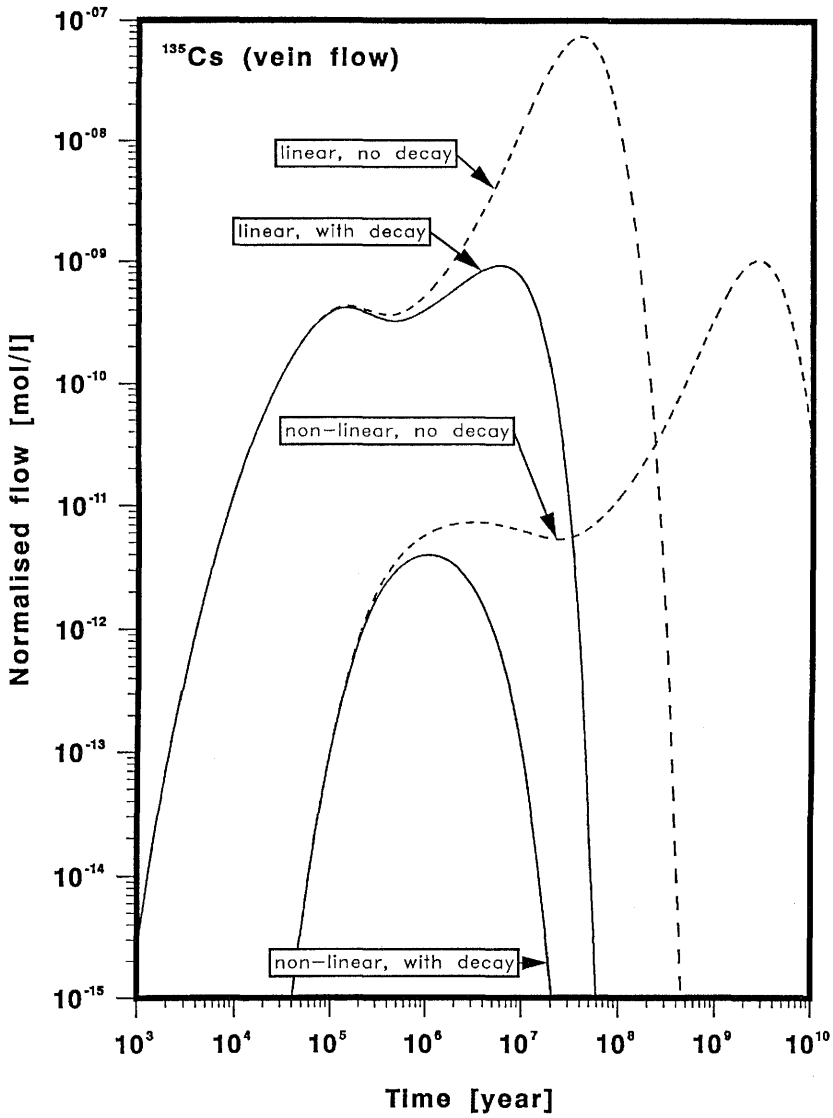

Figure 18: The same as figure 17. The parameters are those for the base case. For the calculation with a linear isotherm, K_d = 0.03 m^3/kg is assumed. The dashed lines are calculations without taking into account radioactive decay and are given for interpretational purposes (see text).

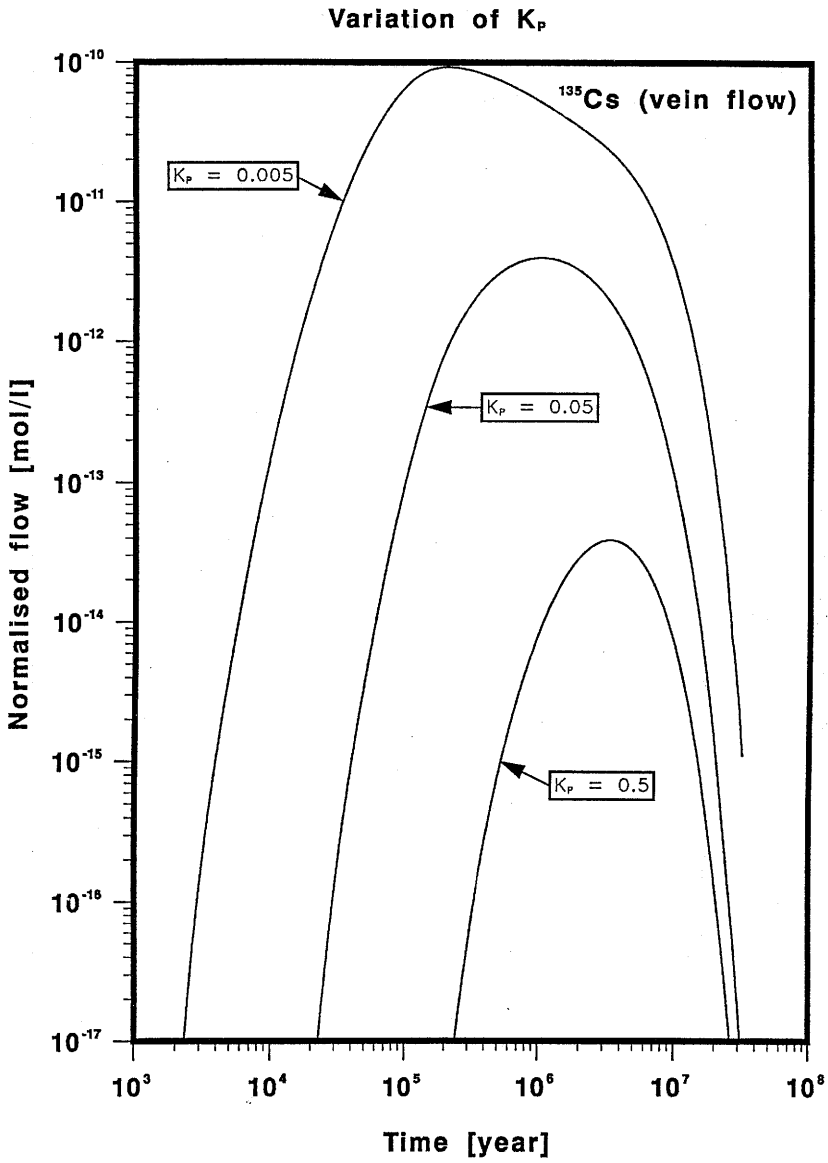

Figure 19: The same as figure 17. The parameters are those of the base case except the Freundlich sorption coefficient K_p [mol$^{0.3}$m$^{2.1}$/kg] whose value is indicated in the figure.

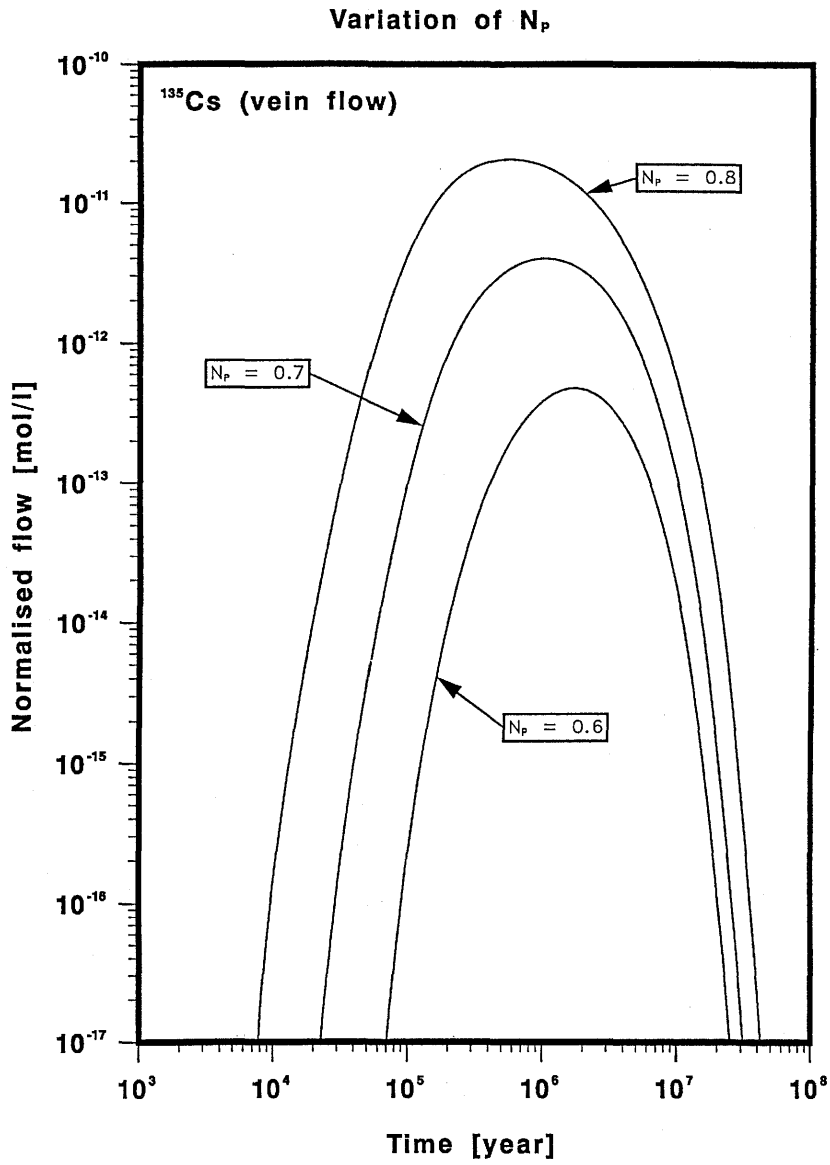

Figure 20: The same as figure 17. The parameters are those of the base case except the Freundlich sorption exponent N_p whose value is indicated in the figure.

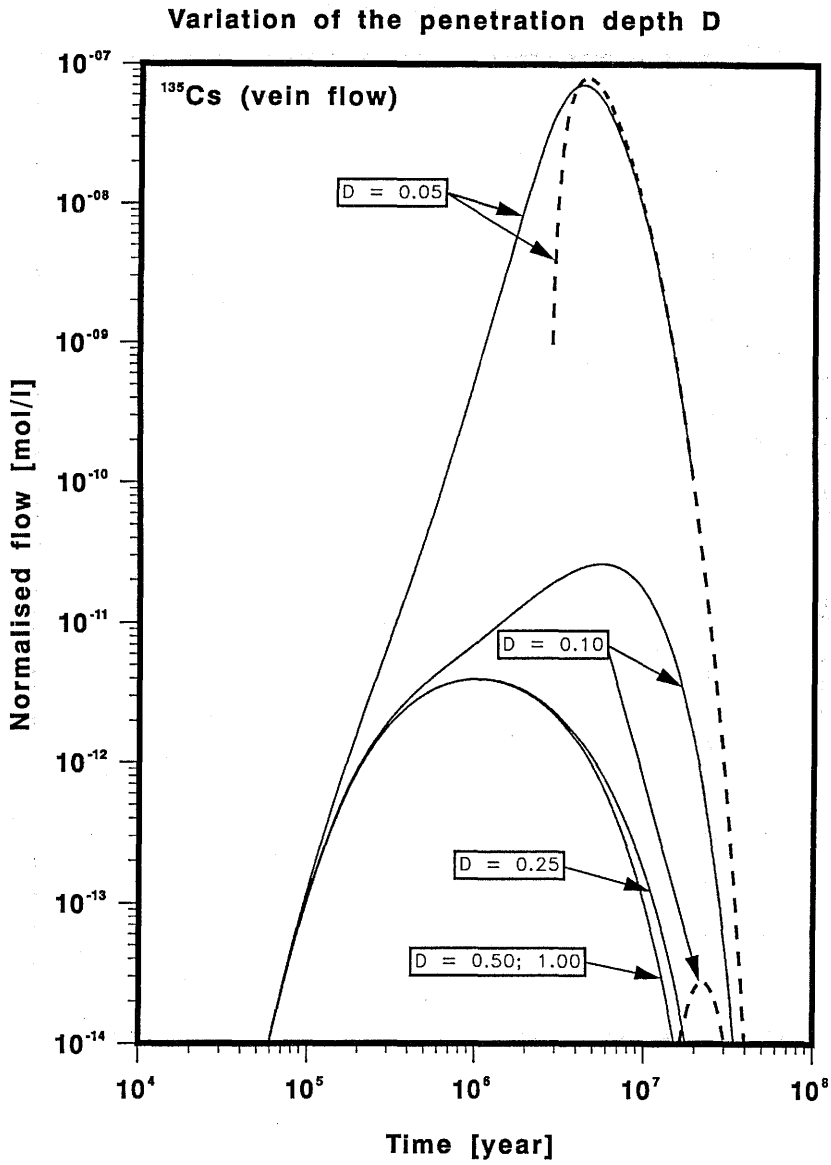

Figure 21: The same as figure 17. The parameters are those of the base case except the maximal penetration depth D [m] into the kakirite matrix, whose values are indicated in the figure. The full lines are the 2D calculations with matrix diffusion, the broken lines 1D calculations with the effective surface sorption approximation.

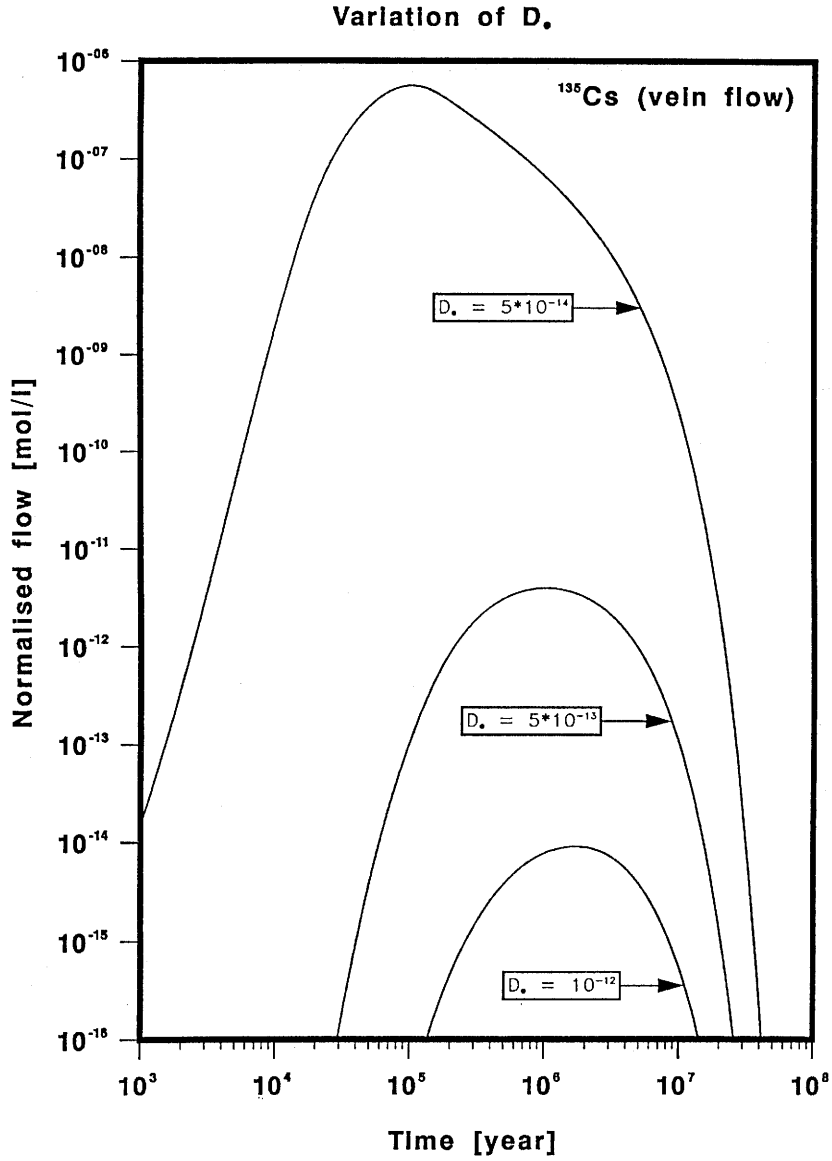

Figure 22: The same as figure 17. The parameters are those of the base case except the effective diffusion constant in the matrix D_e [m^2/s] whose values are indicated in the figure.

5.3 Chain transport in the fracture flow system

In the present work, chain transport is investigated in much less detail than the transport of ^{135}Cs. In fact, in the context of investigations of transport of safety relevant nuclides with non–linear sorption isotherms, the results presented are probably more of a mathematical exercise. The reasons are manifold.

Let us first consider the choice of a relevant nuclide chain. The sorption behaviour of neptunium is extremely complex [25], and we are not aware of an isotherm useful in the present context. As an example we consider the ^{238}U chain with the daughters ^{234}U and ^{230}Th. Very probably, the deep groundwaters are already saturated with uranium, and there would be little uranium release from the repository. Looking at the numbers, we have a natural concentration in granitic groundwater [23] of $1.7 \cdot 10^{-8}$ mol/l, a realistic uranium solubility limit [2] of $2.5 \cdot 10^{-9}$ mol/l and a conservative uranium solubility limit [2] of $2.5 \cdot 10^{-7}$ mol/l. Calculations were done with the value of $2.5 \cdot 10^{-7}$ mol/l, leaving a little space for non–linear sorption behaviour. Reliable uranium isotherms for reducing conditions and the solid phases of interest are not known to the authors. For oxidising conditions, a measured isotherm for uranium(VI) sorption on Swiss granite does exist [19]. For the sake of definiteness we have taken the measured Freundlich exponent and reduced the Freundlich coefficient (Table 2) in order to take into account reducing conditions. At this place we would like to point out a shortcoming of our transport code: It is not possible to take into account the space and time dependent effect of concentration of a migrating isotope on the sorption behaviour of all the other isotopes. For uranium, for example, the natural element concentration C_{min} is determined by ^{238}U, whereas all the other isotopes can be neglected. In the transport calculation for ^{238}U, released from the repository, the effect of C_{min} on sorption is taken into account. But for sorption of ^{234}U the time and space dependent concentration of total ^{238}U determines its sorption (both, natural and repository released contributions).
As a conservative practical approximation we take for ^{234}U a linear isotherm and fix the retardation factor according to the maximum release rate of ^{238}U (see Table 1). With all these assumptions, chain calculations of Figure 23 cannot be much more than a mathematical exercise.

In **Figure 23**, a comparison between calculations with linear isotherms and with a non–linear isotherm for ^{238}U are made. Due to the long half–life and the extended repository release, ^{238}U outflow from the geosphere reaches its maximum corresponding to the solubility limit. Since the K_d for the linear sorption calculation was chosen according to this concentration, the outflow is retarded somewhat more strongly in the non–linear sorption case. The effect however, is small since the non–linearity of sorption is operative over a single decade of concentration values only. The daughters ^{234}U and ^{230}Th have much shorter half–lives, they break–through in radioactive

equilibrium. Their maximum concentration is slightly enhanced in the non–linear sorption case, since the ratio of retardation factors of ^{238}U and ^{234}U is slightly smaller than unity in the peak flow region as a consequence from the approximation mentioned before. This difference also shows the goodness of the approximation and its conservatism.

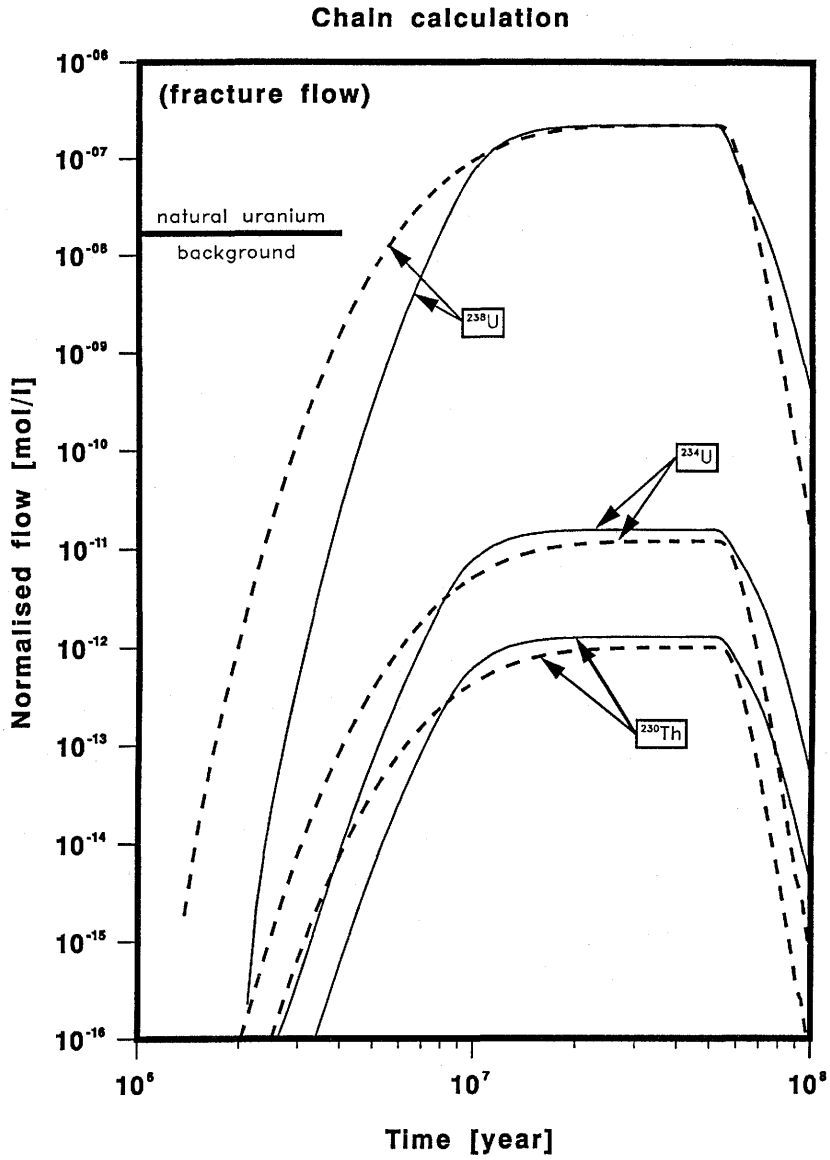

Figure 23: Nuclide flow for the three long–lived members of the ^{238}U chain after a migration distance of 500 m, normalised to a water flow of 4.2 m^3/y, as a function of time after canister failure. Presented are the results for transport in the fractured aplite/pegmatite dykes. The full lines correspond to calculations with a non–linear isotherm for ^{238}U, the dashed lines to a calculation with a linear sorption isotherm.

6 Conclusions

We have presented the governing equations for transport of radionuclides in inhomogeneous dual porosity rocks taking into account non–linear sorption isotherms. The methods to solve these equations and the approaches to verify the ensuing computer code RANCHMDNL have been described.

For the case of a Freundlich isotherm, broad parameter variations based on values for a safety assessment have been performed. Such an isotherm steepens the front of a migrating radionuclide pulse. If transport times are around or larger than nuclide half–lives, only a small portion of the radionuclides survive decay and nuclide outflow from the geosphere is strongly reduced when compared to inflow. In these cases the results are heavily dependent on the parameter values chosen. Especially noted is the change of cesium outflow by five orders of magnitude when the Freundlich exponent is changed by 10 % in the fracture flow calculations. Also, apart from this strong impact, it is evident from the results presented that considering the non–linearity of isotherms reduces the nuclide outflow appreciably when comparing to the standard K_d approach.

For the systems studied the main retardation is produced by matrix diffusion and sorption on inner surfaces. If the available pore volume of rock matrix is sufficiently small and diffusion sufficiently rapid, matrix diffusion can be described by an effective surface sorption.

The fracture flow system ((x,z)–geometry) is much more susceptible to parameter variations than the vein flow system ((r,z)–geometry). This is a consequence of differing dependency of matrix volume on the distance from water carrying zones and the different geometry of the interface between these zones and the rock matrix.
After many years of investigations, the availability of useful and reliable sorption isotherms in the context of safety assessments is still a problem. Cesium is, here, the notable exception.

Work is in progress along different lines. First, general isotherms will be included into the code. This can be done relatively easily by full numerical calculation of the retardation functions based on a tabulation of concentration in the solid versus concentration in the liquid phase. Second, the model is currently being tested through application to results of laboratory experiments (dynamic rock core infiltration and diffusion experiments). Foreseen is also its use in modelling the on–going field migration experiments at NAGRA's Grimsel Test Site. Third, an extension is planned to deal with piecewise constant parameters along a migration path. This will allow modelling of transport through layered systems, be it a series of sediments or a single host rock with spatially varying properties.

7 Appendix:

Numerical Solution of the System of Non–linear Partial Differential Equations

Analytical solutions to the coupled system of eq. (2.7) and (2.9) are known only for very specific retardation functions $R_f(C_f^i)$, $R_p(C_p^i)$, $\tilde{R}_f(C_f^i)$ and $\tilde{R}_p(C_p^i)$ (eq. (2.10) – (2.13)), linear sorption isotherms, and simple boundary conditions. Therefore, it is necessary to solve the system of equations numerically.
In principle, it is possible to get solutions by help of various numerical methods, such as finite elements, finite differences or random walk. Based on the experience [12] we use the method of lines approximation. This method is a powerful tool to approximate the solution of initial value problems for systems of linear and non–linear partial differential equations.
The method of lines is a semidiscretisation procedure where all independent variables but one are discretisised. For every grid point (e.g. in the space domain) one gets one equation, which means that every partial differential equation is converted into a system of ordinary differential equations. This system of ordinary differential equations can then be solved by using standard algorithms. Such standard algorithms are, for example, Eulers's method or the method by Runge–Kutta or various predictor–corrector methods (e.g. by Adams–Moulton, Adams–Bashforth). There are algorithms with automatic control of the step size and for variable orders of the expansion polynomial and procedures which keep truncation errors within a required accuracy. A special method, used here, for solving ordinary differential equations has been developed by Gear [26]. This algorithm is a multistep predictor/corrector method with all the advantages mentioned above and is especially suitable in the treatment of stiff systems such as the coupled transport equations.

Spatial discretisation and the system of finite difference equations

As mentioned before, in the method of lines approximation, the spatial variable is discretisised whereas time is left continuous. First, we have to find a suitable approximation for spatial derivatives. With the abbreviations[7]

$$C_f^i := C \tag{A.1}$$
$$C_p^i := S \tag{A.2}$$

the system of transport equations can be written as

[7]The quantity S, defined here, should not be confused with S, the concentration of sorbed nuclides as used in the previous sections.

$$\frac{\partial}{\partial t}C = \alpha_1 C^{(2)} + \alpha_2 C^{(1)} + \alpha_3 S^{(1)} \Big/ \begin{matrix} |x| = b \\ r = R \end{matrix} + Q_1 \;=\; \mathcal{L}_1(C,S) + Q_1 \tag{A.3}$$

$$\frac{\partial}{\partial t}S \;=\; \beta_1 S^{(2)} + \beta_2 S^{(1)} + Q_2 \;=\; \mathcal{L}_2(S) + Q_2 \tag{A.4}$$

Superscript (2) denotes the second derivative and superscript (1) the first derivative in z, x or r depending on the specific equation at hand (see also eq. (2.7) and (2.9)). $\mathcal{L}_k$ abbreviate the differential operators in space and Q_k denote, again, sink/source terms. The coefficients α_j and β_j may be space and time dependent with:

$$\alpha_1, \alpha_3, \beta_1, \beta_2 \;\geq\; 0 \tag{A.5}$$

$$\alpha_2 \;<\; 0 \tag{A.6}$$

We look for a solution of eq (A.3) in the domain

$$0 \leq z \leq L \quad ;\forall t > 0 \tag{A.7}$$

and of eq. (A.4) in the domain

$$\left.\begin{matrix} b \\ R \end{matrix}\right\} \leq \begin{cases} |x| \leq D & ;\forall t > 0 \quad \text{(for fractures)} \\ r & \quad\quad\quad\quad\;\; \text{(for veins)} \end{cases} \tag{A.8}$$

For the initial condition as well as for the (upstream-/downstream) boundary conditions we refer the reader to section 2. Due to the continuity condition, eq. (2.20), both eq. (A.3) and (A.4) are coupled.

In order to derive the piecewise polynomial approximation for the space dependency of the functions C and S, we replace the two dimensional integration domain by a set of mesh points

in flow direction:

$$\{z\} \;=\; \{z_1 = 0, z_2, ..., z_i, z_{i+1}, ..., z_N = L\} \tag{A.9}$$

and in matrix-diffusion direction:

$$\left\{\begin{matrix} x \\ r \end{matrix}\right\} := \{x\} \;=\; \left\{ x_1 = \begin{cases} b & \text{(for fractures)} \\ R & \text{(for veins)} \end{cases} \;,\; x_2, ..., x_j, x_{j+1}, ..., x_M = D \right\} \tag{A.10}$$

with[8]

[8]We point out that in general the spacings Δz_i, Δx_j i,j = 1,2, ... are not equidistant. The rectangular mesh is sketched below; the mesh points are labelled as indicated in the figure and for simplicity we assume (for the drawing) equidistant increments Δz_i and Δx_j.

$$\Delta z_i = (z_{i+1} - z_i) \tag{A.11}$$
$$\Delta x_j = (x_{j+1} - x_j) \tag{A.12}$$

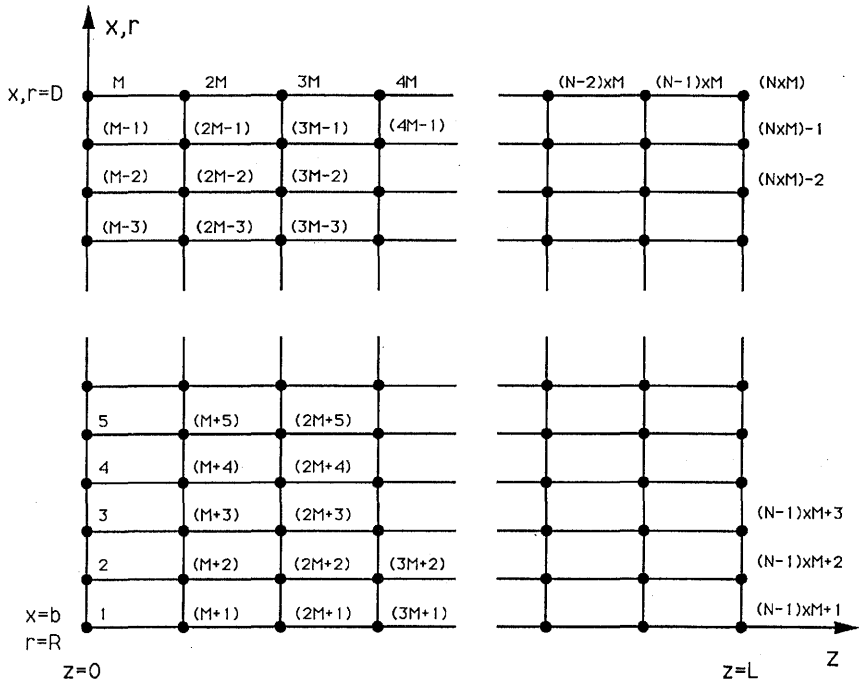

Figure 24: Space mesh system and its numbering.

The transformation of the two coupled partial differential equations into a set of coupled first order ordinary differential equations can be done by Lagrange interpolation techniques.
For a set of given data points $\{u_i,\ v_i\},\ i = 1, 2, ..., n$ and where (u, v) correspond either to (z, C) or (x, S) and with $v_i := v(u_i)$, we get for the $(n-1)$-th order interpolation polynomial P_{n-1}:

$$v(u) \simeq P_{n-1}(u) = \sum_{k=1}^{n} L_k(u) \cdot v_k \tag{A.13}$$

The Lagrange coefficients are given by:

$$L_k(u) = \prod_{\substack{j=1 \\ j \neq k}}^{n} \frac{(u - u_j)}{(u_k - u_j)} \tag{A.14}$$

with $L_k(u_j) = \delta_{kj}$ and $P_{n-1}(u_k) = v_k$. Therefore the approximation polynomial P_{n-1} reproduces exactly the functions C and S at the discretisation points.
For the first derivative we get:

$$v^{(1)}(u) = \sum_{k=1}^{n} L_k^{(1)}(u) \cdot v_k \tag{A.15}$$

where

$$L_k^{(1)}(u) = \sum_{\substack{i=1 \\ i \neq k}}^{n} \frac{\prod_{\substack{l=1 \\ l \neq k,i}}^{n} (u - u_l)}{\prod_{\substack{i=1 \\ i \neq k}}^{n} (u_k - u_i)} \tag{A.16}$$

and for the second derivative:

$$v^{(2)}(u) = \sum_{k=1}^{n} L_k^{(2)}(u) \cdot v_k \tag{A.17}$$

with

$$L_k^{(2)}(u) = \sum_{\substack{i=1 \\ i \neq k}}^{n} \sum_{\substack{m=1 \\ m \neq k,i}}^{n} \frac{\prod_{\substack{l=1 \\ l \neq k,i,m}}^{n} (u - u_l)}{\prod_{\substack{i=1 \\ i \neq k}}^{n} (u_k - u_i)} \tag{A.18}$$

For illustration purposes we assume an equidistant mesh in z and x–direction with increments

$$h_z := \Delta z_i = \text{const.} \quad ; \forall i$$

and

$$h_x := \Delta x_j = \text{const.} \quad ; \forall j. \tag{A.19}$$

For the first derivative, we obtain a second order correct scheme, but with a third order local truncation error:

$$v_1^{(1)} = v^{(1)}(u_1) = \frac{1}{2h}(-3v_1 + 4v_2 - v_3) + O(h^2)$$

$$v_i^{(1)} = v^{(1)}(u_i) = \frac{1}{2h}(-v_{i-1} + v_{i+1}) + O(h^2) \qquad i = 2, 3, ..., (N-1)$$

$$v_N^{(1)} = v^{(1)}(u_N) = \frac{1}{2h}(v_{N-2} - 4v_{N-1} + 3v_N) + O(h^2)$$

and for the second derivative : (A.20)

$$v_1^{(2)} = v^{(2)}(u_1) = \frac{1}{h^2}(v_1 - 2v_2 + v_3) + O(h)$$

$$v_i^{(2)} = v^{(2)}(u_i) = \frac{1}{h^2}(v_{i-1} - 2v_i + v_{i+1}) + O(h^2) \qquad i = 2, 3, ..., (N-1)$$

$$v_N^{(2)} = v^{(2)}(u_N) = \frac{1}{h^2}(v_{N-2} - 2v_{N-1} + v_N) + O(h)$$

In an analogous way, we obtain a fourth order correct scheme for the first derivative with a fifth order local truncation error:

$$v_1^{(1)} = v^{(1)}(u_1) = \frac{1}{12h}(-25v_1 + 48v_2 - 36v_3 + 16v_4 - 3v_5) + O(h^4)$$

$$v_2^{(1)} = v^{(1)}(u_2) = \frac{1}{12h}(-3v_1 - 10v_2 + 18v_3 - 6v_4 + v_5) + O(h^4)$$

$$v_i^{(1)} = v^{(1)}(u_i) = \frac{1}{12h}(v_{i-2} - 8v_{i-1} + 8v_{i+1} - v_{i+2}) + O(h^4) \qquad i = 3, 4, ..., (N-2)$$

$$v_{N-1}^{(1)} = v^{(1)}(u_{N-1}) = \frac{1}{12h}(-v_{N-4} + 6v_{N-3} - 18v_{N-2} + 10v_{N-1} + 3v_N) + O(h^4)$$

$$v_N^{(1)} = v^{(1)}(u_N) = \frac{1}{12h}(3v_{N-4} - 16v_{N-3} + 36v_{N-2} - 48v_{N-1} + 25v_N) + O(h^4)$$

and for the second derivative : (A.21)

$$v_1^{(2)} = v^{(2)}(u_1) = \frac{1}{12h^2}(35v_1 - 104v_2 + 114v_3 - 56v_4 + 11v_5) + O(h^3)$$

$$v_2^{(2)} = v^{(2)}(u_2) = \frac{1}{12h^2}(11v_1 - 20v_2 + 6v_3 + 4v_4 - v_5) + O(h^3)$$

$$v_i^{(2)} = v^{(2)}(u_i) = \frac{1}{12h^2}(-v_{i-2} + 16v_{i-1} - 30v_i + 16v_{i+1} - v_{i+2}) + O(h^4) \qquad i = 3, 4, ..., (N-2)$$

$$v_{N-1}^{(2)} = v^{(2)}(u_{N-1}) = \frac{1}{12h^2}(-v_{N-4} + 4v_{N-3} + 6v_{N-2} - 20v_{N-1} + 11v_N) + O(h^3)$$

$$v_N^{(2)} = v^{(2)}(u_N) = \frac{1}{12h^2}(11v_{N-4} - 56v_{N-3} + 114v_{N-2} - 104v_{N-1} + 35v_N) + O(h^3)$$

Eq. (A.3) and (A.4) can thus be written down for a point (z_i, x_j) using the functional values of $C(z, x, t)$ at neighbouring discretisation points and finally a system of coupled ordinary differential equations of the form results:

$$\frac{\partial C_i(t)}{\partial t} = \sum_{j=1}^{N\text{x}M} V_{ij}(t) \cdot C_j(t) + Q_j(t) \qquad i = 1, 2, ..., (N\text{x}M) \tag{A.22}$$

In the case of a linear sorption isotherm, the coupling matrix V is time-independent, but for non–linear sorption we have to calculate the matrix for every time-step, and in this case the amount of computer time increases dramatically. In general, the structure of V depends not only of the order of the approximation used but also on the arrangement of the mesh points. To illustrate this fact, we use an arrangement as scetched in **Figure 24** and assume a fourth order correct approximation in flow direction with N = 7 discretisation points and also a fourth order correct approximation in the matrix diffusion direction with M = 6 discretisation points. Non–zero elements are indicated by a cross. A typical size of the matrix V may be in the order of 2500 x 2500 matrix elements of which only about 10 % are non–zero. (For larger systems this number may even be smaller.)

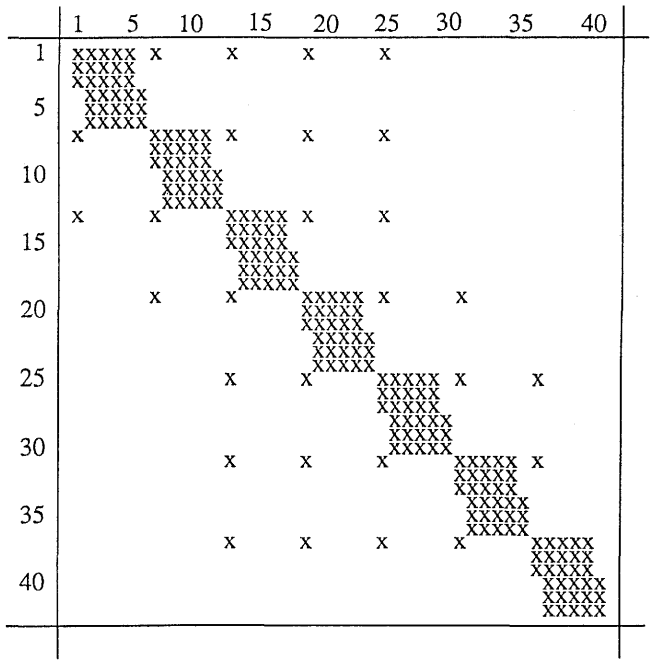

Figure 25: Schematic structure of the coupling matrix V_{ij}. Non zero elements are indicated by a cross.

The order of the approximation in the flow direction determines the number of the upper and lower co–diagonals, whereas the main band stems from the diffusion equation in the rock matrix. From the figure it is easy to see that especially an increase of the order of approximation increases the number of non–zero matrix elements and an increase of the number of discretisation points increases the number of ordinary differential equations.

Time integration

For the numerical time integration of the system of coupled ordinary differential equations we use Gear's method. The reasons are:

- The system of eq. (A.22) is stiff.
- Variable time steps but also variable order approximations are possible.
- During computation local error estimates can be obtained.
- Time discretisation errors are much smaller than spatial discretisation errors because the size of the time steps is restricted by explicit stability conditions.

Whether a system of coupled ordinary differential equations is called stiff depends on the eigenvalues λ_i of the Jacobian. If

$$\max_{1\leq i\leq (N\mathrm{x}M)} \left\{|\lambda_i|\right\} \;>>\; \min_{1\leq i\leq (N\mathrm{x}M)} \left\{|\lambda_i|\right\} \tag{A.23}$$

holds, the system is stiff and stability requirements will force predictor–corrector methods to very small time steps.

As a frame of reference, we give here a brief overview of Gear's method for stiff problems. Consider the system $\dot{y} = f(t, y)$ where y is a vector of length K. For the independent variable t, consider the sequence $t_0 < t_1 < t_2 < .... < t_{n-1} < t_n$, with increment $h = t_n - t_{n-1}$. (The step size h is not necessarily fixed, changes in h are taken into account by interpolation). For stiff problems, the backward differentiation formula is used:

$$\dot{y}_n \;=\; \frac{1}{h\alpha_{n_0}}(y_n - \sum_{k=1}^{q} \alpha_{n_k} y_{n-k}) \tag{A.24}$$

Here, q is the order of the method,[9] the coefficients α_{n_k} are order dependent constants and y_{n-k} are previously calculated values. Let $\dot{y}_n^{(i)}$ and $y_n^{(i)}$ be the predicted values of $\dot{y}_n$ and y_n, resprectively, in the (i)-th iteration.The residuals are

$$\tilde{Q}(y_n^{(i)}) \;=\; (y_n - y_n^{(i)}) - h\alpha_{n_0}(\dot{y}_n - \dot{y}_n^{(i)}) \tag{A.25}$$

[9]In the IMSL routine DGEAR, edition 9, the order is restricted to $1 \leq q \leq 5$.

from which it follows that finding the solution y_n is equivalent to determining the zeros of $\tilde{Q}(y_n^{(i)})$. This is done by a modified Newton iteration:

$$P_n^{(i)}(y_n^{(i+1)} - y_n^{(i)}) = -\tilde{Q}(y_n^{(i)}) \tag{A.26}$$

or:

$$y_n^{(i+1)} = y_n^{(i)} - P_n^{(i)^{-1}}\tilde{Q}(y_n^{(i)}) \quad ; \quad i = 0, 1, 2, ... \tag{A.27}$$

$\mathrm{P}_n^{(i)}$ is a $(K\mathrm{x}K)$-matrix and is given by

$$\begin{aligned} P_n^{(i)} &= \frac{d}{dy_n^{(i)}}\tilde{Q}(y_n^{(i)}) = \frac{d}{dy_n^{(i)}}\left\{y_n - y_n^{(i)} - h\alpha_{n_0}(\dot{y}_n - \dot{y}_n^{(i)})\right\} \\ &= \frac{d}{dy_n^{(i)}}\left\{y_n - y_n^{(i)} - h\alpha_{n_0}\left[\dot{y}_n - (V_n^{(i)}y_n^{(i)} + Q_n^{(i)})\right]\right\} \end{aligned} \tag{A.28}$$

$$P_n^{(i)} = -I + h\alpha_{n_0}\left[\frac{dV_n^{(i)}}{dy_n^{(i)}}y_n^{(i)} + V_n^{(i)} + \frac{dQ_n^{(i)}}{dy_n^{(i)}}\right] = -I + h\alpha_{n_0}J_n^{(i)} \tag{A.29}$$

the expression within the brackets, $J_n^{(i)}$, being the Jacobian matrix of all the derivatives and I is the identity matrix. We would like to point out that, in the case of a linear sorption isotherm, the first term $\frac{dV_n^{(i)}}{dy_n}$ vanishes because V is constant in y (and t) and the third term $\frac{dQ_n^{(i)}}{dy_n}$ is also constant. Therefore one has to evaluate the Jacobian only once, whereas in the case of a non–linear sorption isotherm it is (in principle) necessary to re–evaluate the whole expression for the Jacobian at every time step. We also remark that the derivatives in eq. (A.29) only enter the diagonal elements of J. Since the iteration process is strongly convergent as long as

$$|h\alpha_{n_0}| \cdot \left\|J_n^{(i)}\right\| < 1 \quad ; \forall\, n \quad [10] \tag{A.30}$$

it is not (in practice) necessary to evaluate P at every time step. Moreover, J is only evaluated at those steps where a new value is necessary on the basis of a convergence failure. The step size h and the method's order q are varied in order to stay within local error tolerances. In general, the efficiency of Gear's method is closely related to those of the evaluation of the Jacobian J and the inversion of the matrix P. As mentioned above, the general structure of V, and therefore also of J, is a banded sparse matrix. To handle such matrices efficiently, the Yale sparse matrix solver [27] has been included in the Gear code package.

[10] As norm of a matrix A we define: $||A|| = \max_j \sum_i |A_j^i|$.

The problem of code verification

When developing a code, one of the main tasks is code verification. This implies comparison between numerical results and an analytical solution of the problem, or a benchmarking with other (ideally:verified) codes. The goal is to determine the numerical accuracy of the code. Errors can arise from different sources: round–off errors, numerical instabilities or truncation errors as a result of an inadequate choice of discretisation. The (finite) difference equations only approximate the differential equations, introducing truncation errors which go to zero as dz, dr, dx and dt approach zero. There are no known mathematical criteria for suitable mesh sizes, even for analytically solvable problems; these have to be adjusted every time.
Within the INTRACOIN project [12], there has been an extensive intercomparison of numerical transport codes. There, the extensive results presented from RANCH (a semi–analytical model) and RANCHN (a fully numerical model) calculations compared very well with analytical solutions as well as with numbers from other reliable codes. RANCHN was the starting point for development of RANCHMD, which includes matrix diffusion and linear sorption within the solid rock matrix and onto fracture/vein surfaces [1] and has also been benchmarked within INTRACOIN. Based on this well tested and verified code, the model and also the code have been expanded to include non–linear sorption isotherms, resulting in the code RANCHMDNL.

- As a first verification step for RANCHMDNL, numerical results from RANCHMD had to be reproduced exactly. For this test, the Jacobian (see eq. (A.29)) has to be calculated only once. Also the derivatives of the source/sink terms enter the formalism only as a constant.

- In a further step, we reproduced the so called 'quasi–linear case'. This means, we assumed a non–linear Freundlich isotherm (within the fracture/vein as well as in the matrix) but with an exponent close to unity. The Jacobian is not constant anylonger, resulting in increased CPU–time and slightly changed step sizes for the time integration, but exactly the same results as RANCHMD were obtained. (Of course, we tested both alternative geometries for single nuclides and for nuclide decay chains.)

- In 1983 numerical results of the one–dimensional transport equation neglecting matrix diffusion but including non–linear sorption effects were presented [4]. The code, based on the pseudospectral method, used Chebyshev polynomials for the expansion of C and its derviatives instead of the Lagrange approximation. By putting the effective diffusion constant $\epsilon_p D_p$ to zero and thus neglecting diffusive transport into the matrix, we simulated the one–dimensional problem and satisfactorily reproduced the old results within a few percent. Rough qualitative comparisons were also made with results presented in ref. [6].

- To check whether the non–linearity is also correctly incorporated into the diffusion equation, we made use of the concept of the effective sorption approximation. Again, we obtained complete numerical agreement between both, one– and two–dimensional calculations.

We finish this section with the remark that we have not currently available another code which can produce numerical solutions of the two-dimensional transport equation as presented in this report. Therefore, in spite of the successful verification tests we have carried out, a strict and inexorable verification of our code is still missing.

Acknowledgements

This work has profited from discussions with many colleagues. Special thanks are due to B. Baeyens, M. Bradbury, R. Grauer, F. Herzog, I. McKinley, T. Melnyk, P. Smith, F. van Dorp and P. Zuidema for discussions, S. Aksoyoglu, B. Ruegger and T.T. Vandergraaf for providing us with sorption data, C. Degueldre and F. Sarott for the translation of abstracts, and H.P. Alder, R. Brogli and C. McCombie for their interest in this work. Partial financial support by NAGRA is gratefully acknowledged. We are deeply indebted to Mrs. R. Bercher for her tireless efforts in typing the manuscript.

References

[1] **Hadermann, J. and Roesel, F.:** "Radionuclide Chain Transport in Inhomogeneous Crystalline Rocks – Limited Matrix Diffusion and Effective Surface Sorption", EIR–Bericht Nr. 551, Würenlingen 1985 and NTB 85–40, NAGRA, Baden, February 1985

[2] Project Gewähr 1985; "Nuclear waste management in Switzerland: Feasibility studies and safety analyses", NGB 85–09, NAGRA, Baden, June 1985

[3] Sediment Study – Intermediate report 1988, Disposal Options for Long Lived Radioactive Waste in Swiss Sedimentary Formations, Executive Summary, NTB 88–25E, NAGRA, Baden, July 1989

[4] **Hadermann, J., Roesel, F.:** "Numerical Solution of the Radionuclide Transport Equation – Non–linear Sorption Effects", EIR–Bericht Nr. 506, Würenlingen 1983 and NTB 83–23, Baden, November 1983

[5] **Grove, D.B. and Stollenwer, K.G.:** "Computer Model of One–Dimensional Equilibrium Controlled Sorption Processes", US GS Water Resources Investigations Report 84–4-095, Denver 1984

[6] **Melnyk, T.W.:** "Effects of Sorption Behaviour on Contaminant Migration", AECL – 8390, Pinawa, Manitoba, November 1985

[7] **Flühler, H., Jury, W.A.:** "Estimating Solute Transport Using Nonlinear, Rate Dependent, Two Site Adsorption Models", Swiss Federal Institute of Forestry Research, Report Nr. 245, Birmensdorf, 1983

[8] **Bear, J.:** "Hydraulics of Groundwater", McGraw–Hill Book Company, 1979

[9] **Bear, J.; Verruijt, A.:** "Modelling Groundwater Flow and Pollution", D. Reidel Publishing Company, Dordrecht, Holland, 1987

[10] **Neretnieks, I.:** Journal of geophyscial research, Vol. 85, No. B8 (1980), p. 4379 – 4397.

[11] **Rae, J., Lever, D.A.:** "Will diffusive retention delay radionuclide movement underground?", Report TP.853, AERE Harwell, July 1980

[12] INTRACOIN: "International nuclide transport code intercomparison study", Final reports level 1, Stockholm, September 1984, and levels 2 and 3; Stockholm, May 1986

[13] **Kinniburgh, D.G.:** "General Purpose Adsorption Isotherms", Environ. Sci. Technol., Vol. 20 (1986), P. 895 – 904

[14] **van Genuchten, M.Th., Davidson, J.M., Wierenga, P.J.:** "An Evaluation of Kinetic and Equilibrium Equations for the Prediction of Pesticide Movement through Porous Media", Soil Sci. Soc. Am. Proc., Vol. 38 (1974), p. 29 – 35

[15] **Travis, C.C. and Etnier, E.L.:** "A Survey of Sorption Relationships for Reactive Solutes in Soil", J. Environ. Qual., Vol. 10 (1981), p. 8

[16] **Foster, S.S.D.:** "The Chalk Groundwater Tritium Anomaly – A Possible Explanation", J. Hydrol., Vol. 25 (1975), p. 159

[17] **Neretnieks, I.:** "Age Dating of Groundwater in Fissured Rock: Influence of Water Volume in Micropores", Water Res. Res. Vol. 17 (1981), p. 421

[18] **Sudicky, E.A. and Frind, E.O.:** "Carbon 14 Dating of Groundwater in Confined Aquifers: Implications of Aquitard Diffusion", Water Res. Res. Vol. 17 (1981), p. 1060

[19] **Aksoyoglu, S., Bajo, C., Mantovani, M.:** "Sorption of U(VI) on granite", J. Radioanal. Nucl. Chem. Vol. 134 (1989), no. 2

[20] **Aksoyoglu, S., Baeyens, B., Bradbury, M., Mantovani, M.:** "Batch sorption experiments with iodine, bromine, strontium, sodium and cesium on Grimsel mylonite", PSI–Report and NAGRA technical report, in preparation.

[21] **Bischoff, K., Wolf, K., Heimgartner, B.:** "Hydraulische Leitfähigkeit, Porosität und Uranrückhaltung von Kristallin und Mergel: Bohrkern–Infiltrationsversuche", EIR–Bericht Nr. 628, Würenlingen 1987 and NTB 85–42, NAGRA, Baden, April 1987

[22] **Hartley, R.W.:** " Release of radionuclides to the geosphere from a repository for high–level waste – Mathematical model and results", EIR–Report, Nr. 554, Würenlingen, 1985 and NTB 85–41, Baden, 1985

[23] NAGRA (1989): Hydrochemische Analysen – Unpubl. internal Report, Nagra, Baden (Gautschi, A.: private communication)

[24] **Wittwer, C:** "Sondierbohrungen Böttstein, Weiach, Riniken, Schafisheim, Kaisten, Leuggern; Probenahmen und chemische Analysen von Grundwässern aus den Sondierbohrungen", NTB 85–49, Baden, Oktober 1986

[25] **Meyer, R.E., Arnold, W.D., Case, F.I.:** "Valence Effects on the Sorption of Nuclides on Rocks and Minerals", NUREG/CR–3389, ORNL–5978, Oak Ridge, TN, 1984

[26] **Gear, C.W.:** "Numerical Initial Value Problems in Ordinary Differential Equations", Prentice–Hall, Inc., Englewood Cliffs, New Jersey 1971

[27] **Eisenstat, S.C., Gursky, M.C., Schultz, H.M. Sherman, A.H.:**"Yale sparse matrix package", Research report No. 112 and 114, Department of computer science, Yale University, 1977